Supporting Information

for

Platinum(II) Complexes of Benzannulated N^N⁻^O-Amido Ligands: Bright Orange Phosphors With Long-Lived Excited States

Issiah B. Lozada,[a] J. A. Gareth Williams,[b,] and David E. Herbert[a,*]*

[a] Department of Chemistry and the Manitoba Institute for Materials, University of Manitoba, 144 Dysart Road, Winnipeg, Manitoba, R3T 2N2, Canada;

*david.herbert@umanitoba.ca

[b] Department of Chemistry, Durham University, Durham, DH1 3LE, UK;

*j.a.g.williams@durham.ac.uk

Table of Contents

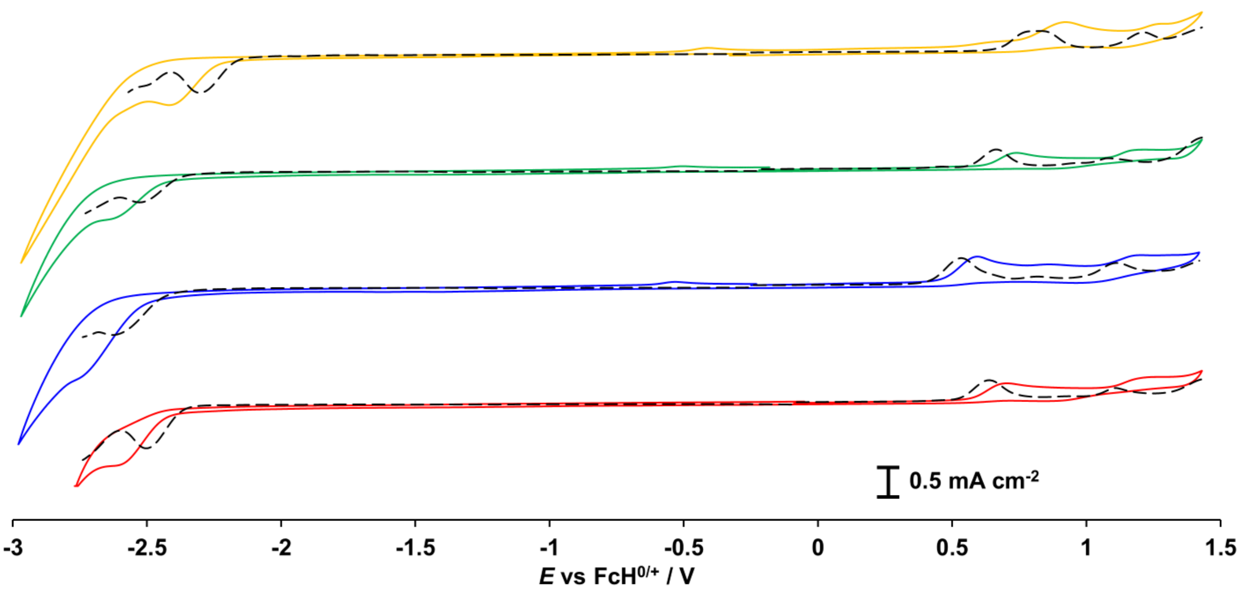

Figure S1. Cyclic voltammograms (**—**) and differential pulse voltammograms (---) of **L1-L4** in CH_2Cl_2 with 0.1 mM of $[NBu_4][PF_6]$ as the supporting electrolyte, glassy carbon as the working electrode, and Pt wire as the counter electrodes. CV scan rates were 100 mV/s. Potentials are listed vs. $FcH^{0/+}$ redox couple (FcH = ferrocene).

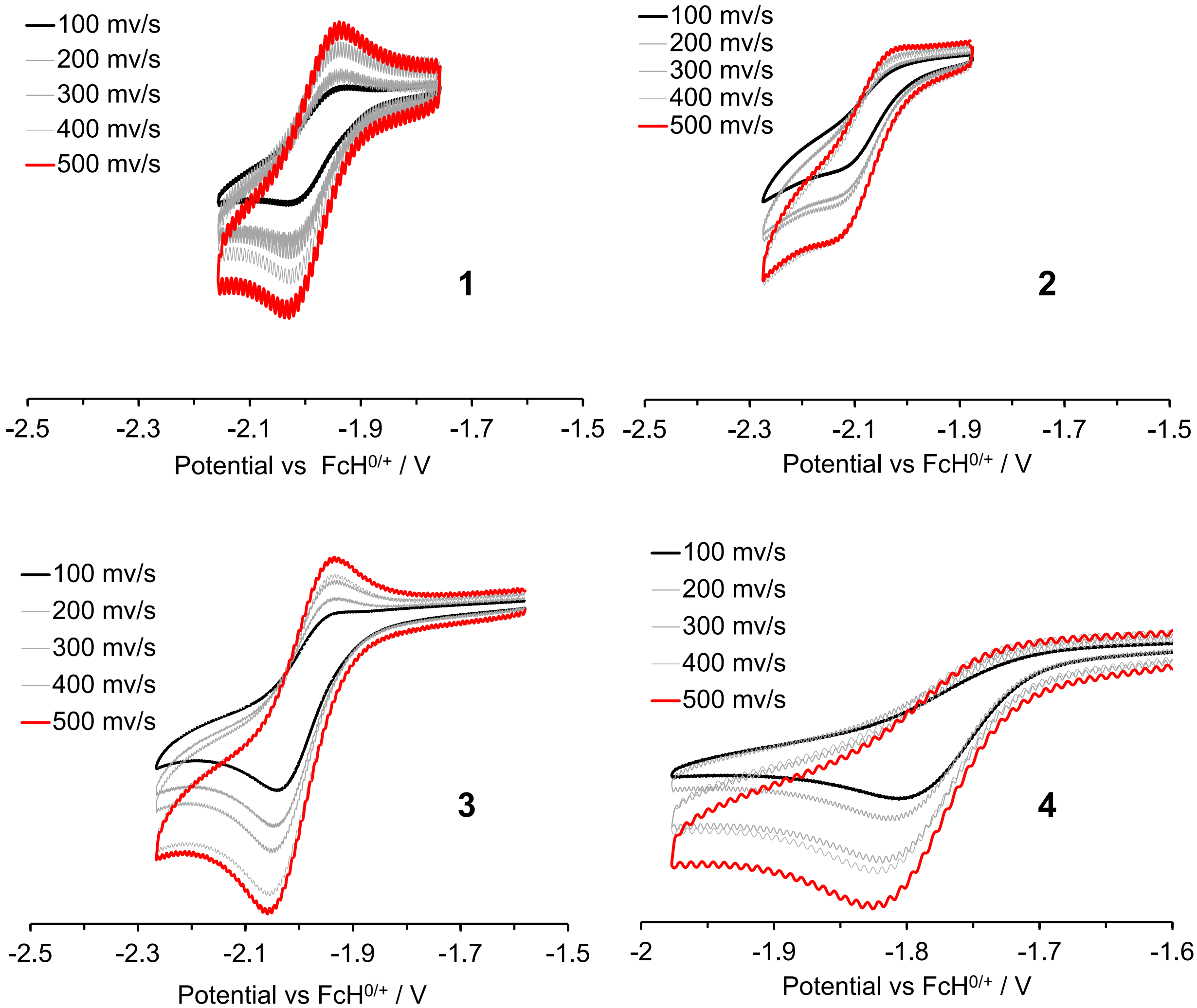

Figure S2. Scan rate dependence of cathodic events for **1-4**.

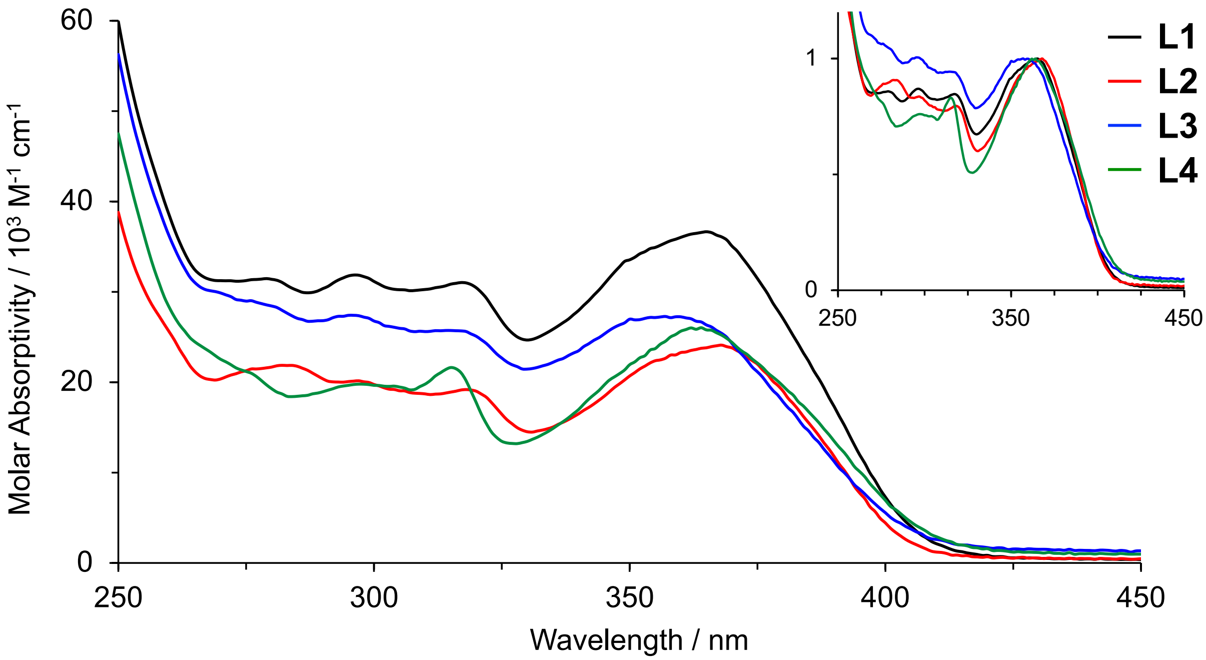

Figure S3. UV-Vis spectra of **L1**-**L4** in CH_2Cl_2 at 298 K. Inset shows normalized spectra.

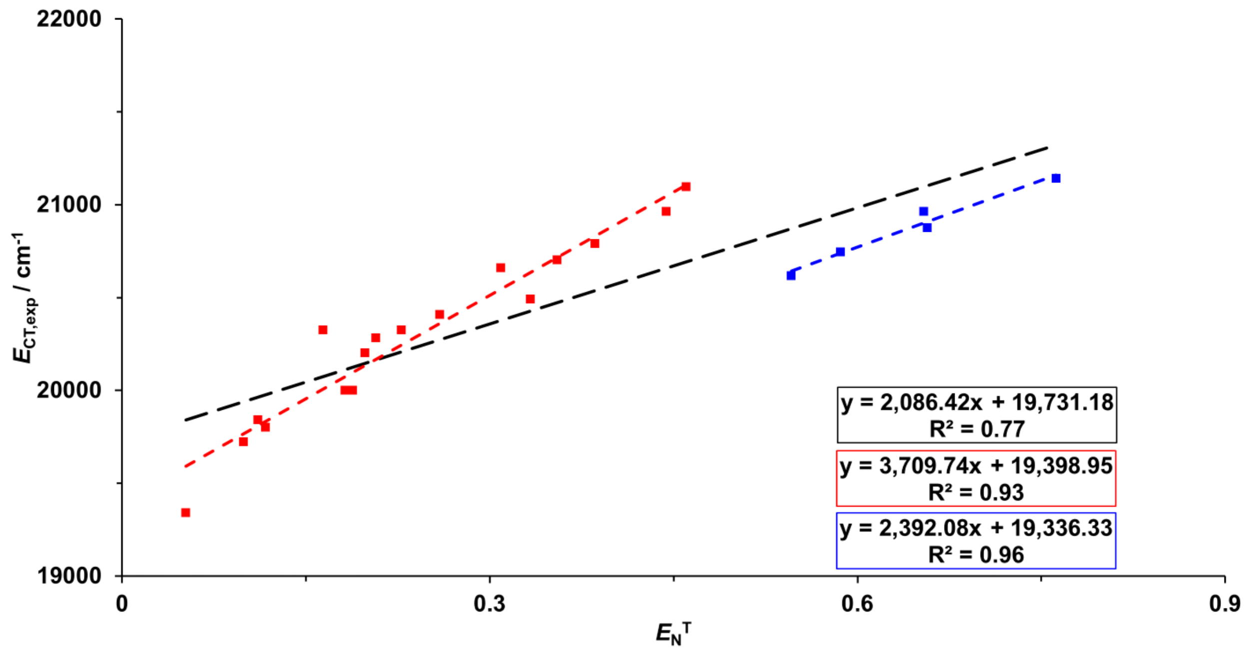

Figure S4. Correlation between $E_{CT,exp}$ (cm^{-1}) on Reichardt's solvent E_N^T parameters with aprotic and protic solvents treated together (---), and protic (---) and aprotic (---) solvents treated separately.

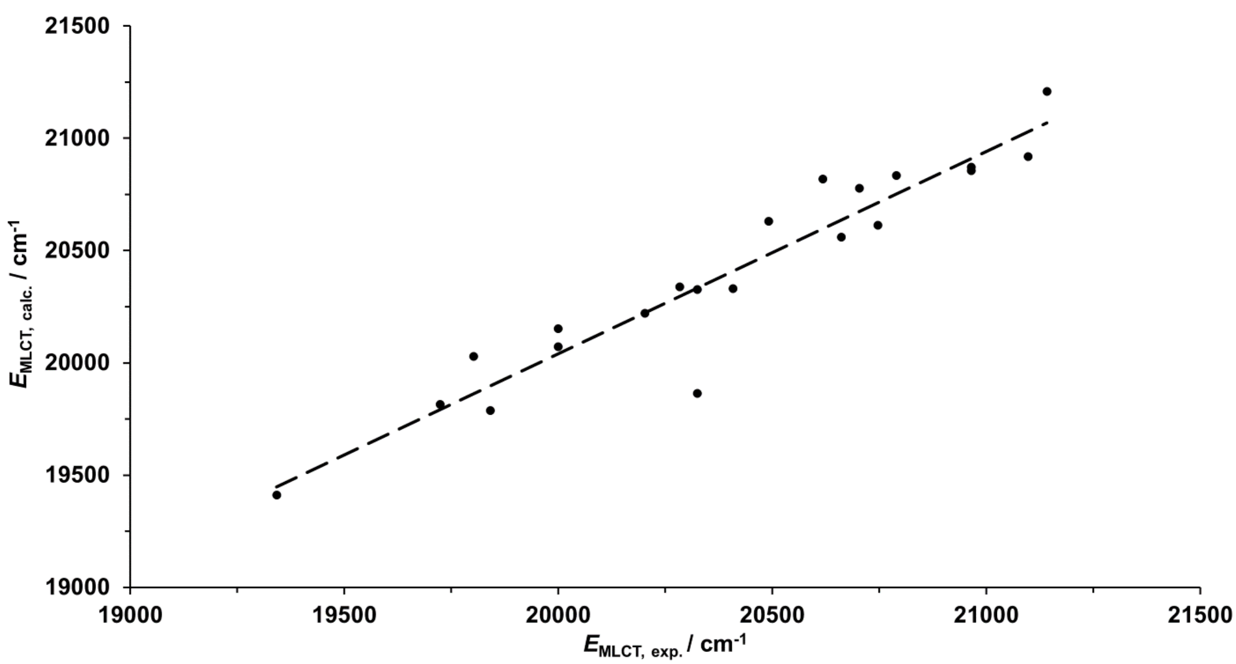

Figure S5. Correlation between $E_{CT,exp.}$ (cm^{-1}) and $E_{CT,calc.}$ (cm^{-1}) calculated using Catalan's multiparameter solvent approach.

Table S1. Reichardt's E_N^T and Catalan solvent (SP, SdP, SA and SB) parameters for **4**.

Solvent	$\lambda_{abs,CT}$/nm	E_{CT}/cm^{-1}	SP	SdP	SA	SB	E_N^T
CCl_4	517	19342	0.768	0	0	0.044	0.052
benzene	504	19841	0.793	0.27	0	0.124	0.111
toluene	507	19724	0.782	0.284	0	0.128	0.099
$CHCl_3$	490	20408	0.783	0.614	0.047	0.071	0.259
Et_2O	505	19802	0.617	0.385	0	0.562	0.117
anisole	495	20202	0.82	0.543	0.084	0.299	0.198
CH_2Cl_2	484	20661	0.761	0.769	0.04	0.178	0.309
ClPh	500	20000	0.833	0.537	0	0.182	0.188
BrPh	500	20000	0.875	0.497	0	0.192	0.182
THF	493	20284	0.714	0.634	0	0.591	0.207
acetone	483	20704	0.651	0.907	0	0.475	0.355
DMF	481	20790	0.759	0.977	0.031	0.613	0.386
CH_3CN	474	21097	0.645	0.974	0.044	0.286	0.46
DMSO	474	21097	0.83	1	0.072	0.647	0.444
CNPh	488	20492	0.851	0.852	0.047	0.281	0.333
EtOAc	492	20325	0.656	0.603	0	0.542	0.228
*i*ProH	485	20619	0.633	0.808	0.283	0.83	0.546
1-BuOH	482	20747	0.674	0.655	0.341	0.809	0.586
CH_3OH	473	21142	0.608	0.904	0.605	0.545	0.762
EtOH	477	20964	0.633	0.783	0.4	0.658	0.654
2OMeEtOH	479	20877	-	-	-	-	0.657

Table S2. Catalan solvent parameter coefficients and statistics obtained from linear regression.

Regression Statistics			Coefficients	Standard Error	t statistic	P-value
Multiple R	0.974	**Intercept**	19619	368	53.326	0.000
R Square	0.948	**SP**	-402	452	-0.890	0.387
Adjusted R Square	0.935	**SdP**	1649	133	12.382	2.81E-09
Standard Error	130.4	**SA**	774	220	3.517	0.003
Observations	20	**SB**	-151	176	-0.860	0.403

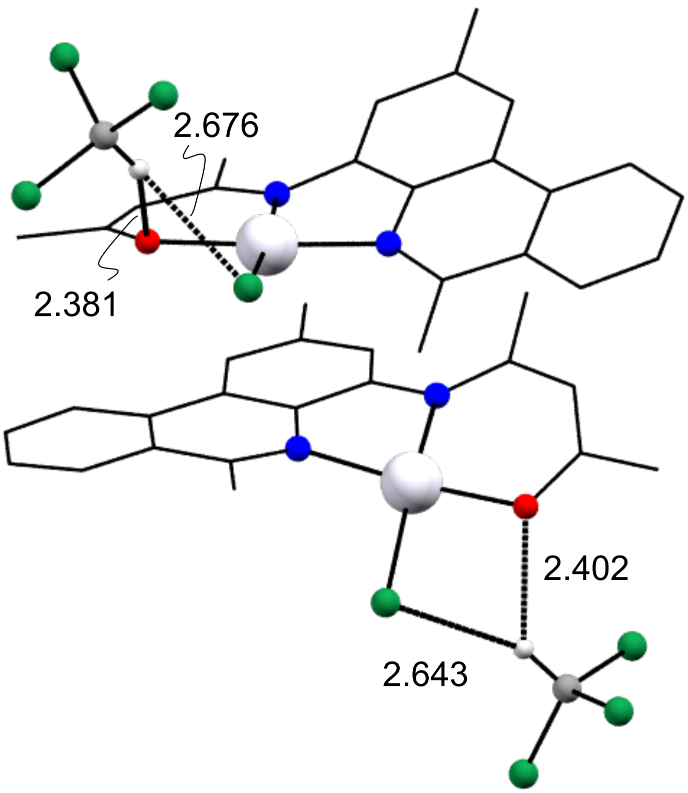

Figure S6. Solid-state structure of **4** showing hydrogen bonding interaction with co-crystallized $CHCl_3$ solvent molecules.

Estimation of empirical HOMO-LUMO energies from UV-Vis absorbance and cyclic voltammetry

Following a similar procedure employed Pan and co-workers[1], we estimated the HOMO and LUMO energies using the following equations:

$$E_{HOMO} = -(E_{onset,ox} + 4.8 - E_{FcH}) \qquad (1)$$

$$E_{LUMO} = -(E_{onset,red} + 4.8 - E_{FcH}) \qquad (2)$$

where E_{HOMO} and E_{LUMO} are the HOMO and LUMO energies, $E_{\mathrm{onset,ox}}$ and $E_{\mathrm{onset,red}}$ are the onset oxidation and reduction potentials estimated using DPV, 4.8 is the reference energy level of ferrocene (FcH, 4.8 eV below the vacuum level), and E_{FcH} is the FcH $^{0/+}$ potential vs. Ag/AgCl similarly estimated with DPV. Electrochemical parameters and experimentally derived HOMO-LUMO energies and gaps are summarized in Table 1. To corroborate the parameters and trends obtained from electrochemistry, we also estimated the optical gap (E_{g}) from the UV-Vis spectra of all compounds. This can be estimated from the following equation

$$E_g = \frac{hc}{\lambda_{onset}} \qquad (3)$$

where h is Planck's constant, c is the speed of light in vacuum, and λ_{onset} is the onset of the UV-Vis spectra. We introduce a modification to equation (3) for the Pt(II) complexes. TDDFT analyses (see below) reveal that the lowest energy manifold can largely be assigned to HOMO→LUMO transitions leading to

$$E_g = \frac{hc}{\lambda_{max}} \qquad (4)$$

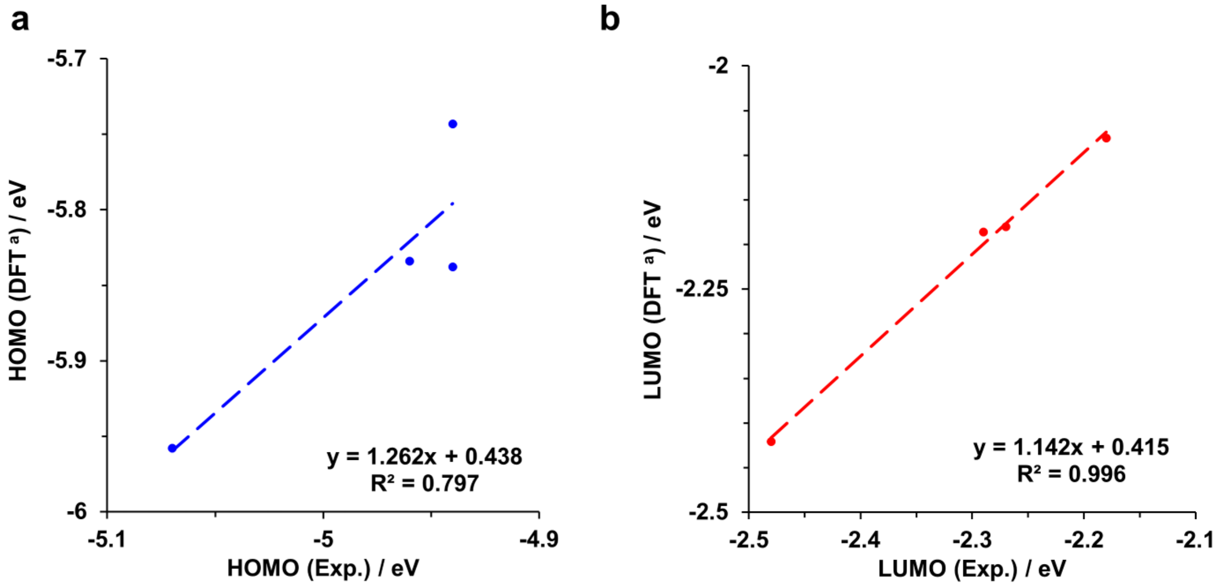

Figure S7. Correlation between experimentally and computationally derived (a) HOMO and (b) LUMO energies of **1-4**.

Table S3. Select optimized structural parameters for the ground state ($^1GS_{eq}$) **1-4** (RIJCOSX-rPBE0-D3(BJ)/def2-TZVP(-f)+def2/J).

Bond / Å	1	2	3	4
Pt─N1	1.984	2.025	1.978	1.978
Pt─N2	2.015	1.998	1.991	2.012
Pt─O	1.984	1.986	1.979	1.981
Pt─Cl	2.318	2.319	2.314	2.314
Angle / °				
N1─Pt─N2	82.2	81.8	82.7	82.0
N1─Pt─O	178.5	173.1	178.5	176.1
N1─Pt─Cl	94.8	100.6	95.3	95.2
N2─Pt─O1	96.6	94.6	97.6	96.5
N2─Pt─Cl	176.7	169.6	178.7	176.0
O─Pt─Cl	86.1	84.1	84.4	86.6

Table S4. Select optimized structural parameters for the lowest excited triplet state of **1-4** (RIJCOSX-uPBE0-D3(BJ)/def2-TZVP(-f)+def2/J).

Bond / Å	1	2	3	4
Pt─N1	1.983	2.018	1.984	1.981
Pt─N2	1.994	1.976	1.992	1.982
Pt─O	1.985	1.987	1.983	1.986
Pt─Cl	2.288	2.291	2.287	2.276
Angle / °				
N1─Pt─N2	82.1	81.8	82.3	82.2
N1─Pt─O	178.4	175.3	178.0	178.2
N1─Pt─Cl	95.8	100.2	95.7	95.8
N2─Pt─O1	96.8	95.0	96.6	96.5
N2─Pt─Cl	177.5	168.0	177.6	176.0
O─Pt─Cl	85.4	83.6	85.5	85.6

Table S5. Fragment contributions to the ground state MOs of **1**.

MOs	*E*/eV	Pt	Cl	HC=N	Ar^{phen}	NAcAc	CH_3
L+4	-0.228	43	13	8	19	17	1
L+3	-0.254	10	3	7	62	15	4
L+2	-1.118	4	0	6	52	37	0
L+1	-1.534	3	0	7	69	20	1
L	-2.186	2	0	28	51	17	1
H	-5.834	18	9	1	23	48	0
H-1	-6.663	32	0	15	39	11	2
H-2	-6.851	39	32	1	14	13	1
H-3	-6.945	19	0	3	70	7	1
H-4	-6.966	59	21	2	10	7	0

Table S6. Fragment contributions to the ground state MOs of **2**.

MOs	*E*/eV	Pt	Cl	$(CH_3)C{=}N$	Ar^{phen}	NAcAc	CH_3
L+4	-0.191	9	2	8	68	9	4
L+3	-0.32	40	11	7	13	29	1
L+2	-1.141	6	1	6	57	30	0
L+1	-1.536	4	0	7	62	25	1
L	-2.081	2	0	31	50	15	1
H	-5.743	20	8	2	23	46	0
H-1	-6.553	38	12	14	21	14	1
H-2	-6.683	40	32	2	13	12	1
H-3	-6.83	12	10	5	68	3	2
H-4	-6.918	80	3	3	8	6	0

Table S7. Fragment contributions to the ground state MOs of **3**.

MOs	*E*/eV	Pt	Cl	HC=N	Ar^{phen}	NAcAc	*t*Bu
L+4	-0.227	44	13	8	16	13	1
L+3	-0.259	8	2	7	65	12	4
L+2	-1.116	4	0	6	52	32	1
L+1	-1.535	3	0	6	68	18	2
L	-2.18	2	0	29	50	15	1
H	-5.838	19	9	1	23	41	0
H-1	-6.669	34	0	15	37	8	2
H-2	-6.855	39	32	1	16	11	1
H-3	-6.936	13	0	4	74	5	2
H-4	-6.965	65	20	2	6	3	0

Table S8. Fragment contributions to the ground state MOs of **4**.

MOs	*E*/eV	Pt	Cl	HC=N	Ar^{phen}	NAcAc	CF_3
L+4	-0.293	50	15	8	6	21	0
L+3	-0.671	2	0	3	70	20	6
L+2	-1.27	5	1	8	51	35	1
L+1	-1.712	2	0	6	73	17	1
L	-2.421	2	0	28	52	16	2
H	-5.958	21	10	1	20	47	0
H-1	-6.808	46	4	11	21	18	0
H-2	-6.947	38	35	2	13	12	0
H-3	-7.057	78	7	2	4	7	0
H-4	-7.115	40	39	4	9	7	0

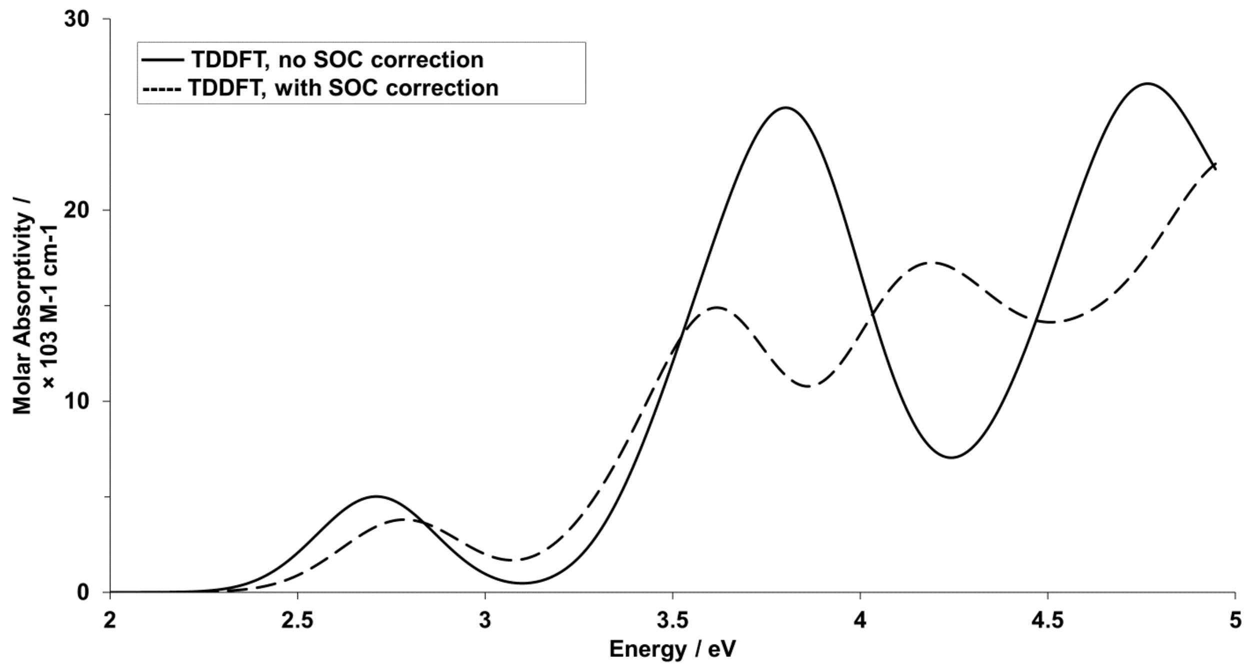

Figure S8. Effects of inclusion of spin-orbit coupling on the calculated UV-Vis absorption spectra of **4**.

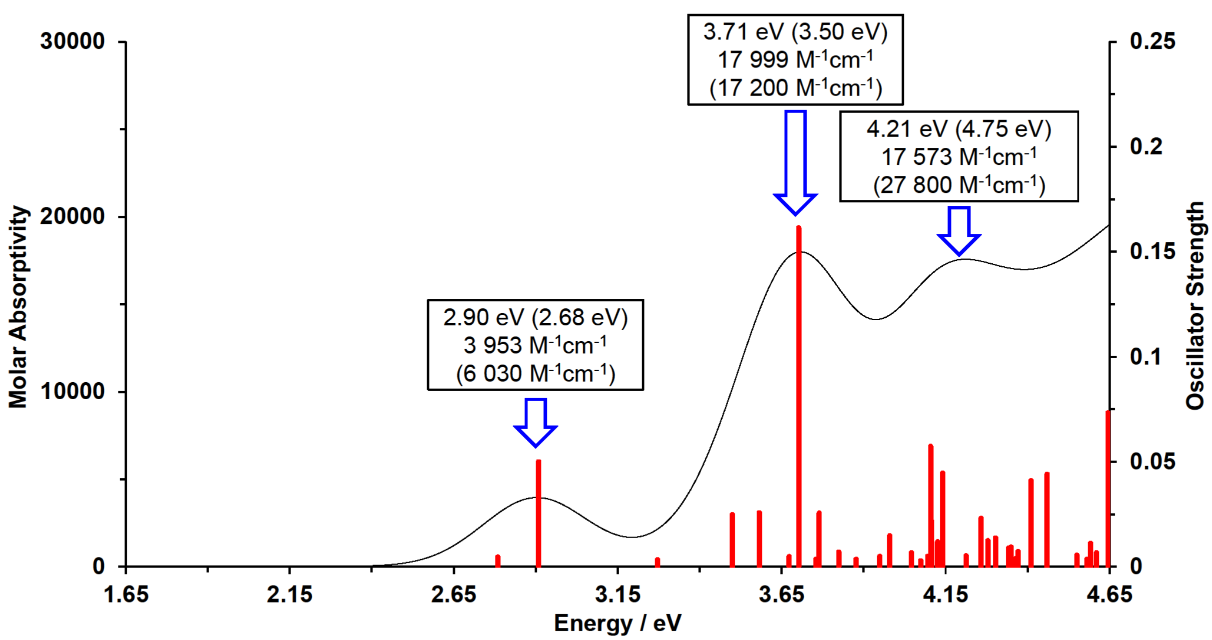

Figure S9. TDDFT simulated SOC-corrected spectrum (—), vertical excitations (—), and oscillator strengths of **1** in CH_2Cl_2. Calculated energies and molar absorptivities ($M^{-1}cm^{-1}$) at each peak maxima are shown with experimental (in parentheses).

Table S9. Spin-only and SOC-corrected TDDFT predicted singlet-singlet, singlet-triplet, and singlet-SOC vertical excitation energies (f > 0.003), MO contributions (>10%), singlet/triplet contributions (>5 %) for **1**. Entries in red reflect SOC calculated transitions which appear in valley regions of the absorption spectrum.

^1S_n	**E/eV**	**f_{osc}**	**MO contributions (> 10%)**	
1	2.82	0.069	H->L (97%)	
2	3.52	0.047	H->L+1(75%), H-1->L (12%)	
3	3.71	0.088	H-1->L (43%), H-2->L (40%)	
4	3.72	0.025	H-2->L (35%), H-4->L (34%), H-1->L (13%)	
5	3.77	0.011	H-4->L (28%), H-3->L (19%), H->L+2 (15%), H-2->L (12%)	
^3T_n	**E/eV**	**f_{osc}**	**MO contributions (> 10%)**	
1	2.21	0.000	H->L (65%), H->L+1 (12%)	
2	2.67	0.000	H-1->L (61%)	
3	3.08	0.000	H->L+1 (45%), H->L (26%), H->L+2 (13%)	
4	3.23	0.000	H-3->L (30%), H->L+2 (20%)	
5	3.32	0.000	H->L+4 (41%), H-2->L+4 (13%), H->L+3 (11%), H-3->L (10%)	
6	3.43	0.000	H-1->L (19%), H-3->L (18%), H-3->L+1 (18%), H->L+2 (14%)	
7	3.50	0.000	H-3->L (19%), H-1->L+1 (18%), H->L+2 (12%)	
8	3.56	0.000	H-2->L (64%)	
9	3.68	0.000	H-4->L (61%), H-5->L (11%), H-3->L (10%)	
10	3.72	0.000	H-1->L+2 (25%), H-3->L+1 (17%), H->L+2 (10%)	
11	3.80	0.000	H-4->L+4 (22%), H-1->L+4 (16), H-3->L+4 (11%), H-4->L (10%)	
SOC	**E/eV**	**f_{osc}**	**^1S_n contributions (> 5%)**	**^3T_n contributions (> 5%)**
4	2.79	0.005	1 (6%)	2 (90%)
7	2.91	0.050	1 (85%)	2 (5%), 9 (6%)
13	3.27	0.003	4 (31%), 5 (38%)	3 (11%)
20	3.50	0.025	2 (18%), 3 (18%)	6 (8%), 9 (25%), 11 (9%)
24	3.58	0.026	2 (16%), 3 (17%), 5 (10%)	6 (8%), 9 (13%), 11 (6%), 12 (6%)
28	3.68	0.005	-	7 (62%), 10 (7%), 12 (8%), 13 (8%)
30	3.70	0.161	2 (14%), 4 (13%), 6 (10%)	7 (5%), 9 (16%), 10 (5%), 11 (5%)

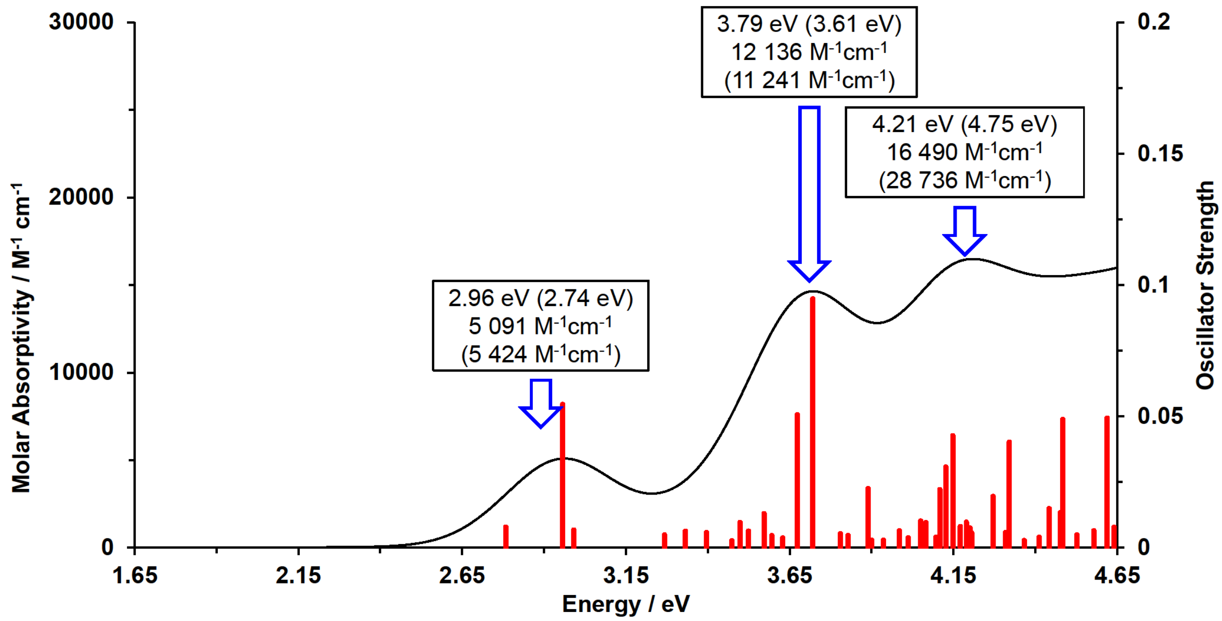

Figure S10. TDDFT simulated SOC-corrected spectrum (—), vertical excitations (—), and oscillator strengths of **2** in CH_2Cl_2. Calculated energies and molar absorptivities (M^{-1} cm^{-1}) at each peak maxima are shown with experimental (in parentheses).

Table S10. Spin-only and SOC-corrected TDDFT predicted singlet-singlet, singlet-triplet, and singlet-SOC vertical excitation energies (f > 0.003), MO contributions (>10%) and singlet/triplet contributions (>5 %) for **2**. Entries in red reflect SOC calculated transitions which appear in valley regions of the absorption spectrum.

$^{1}S_{n}$	E/eV	f_{osc}	MO contributions (> 10%)
1	2.84	0.078	H->L (97%)
2	3.36	0.067	H->L+1 (67%), H->L+2 (12%)
3	3.63	0.048	H-1->L (44%), H->L+2 (22%), H->L+1 (15%)
4	3.64	0.018	H-2->L (27%), H-1->L (19%), H->L+2 (19%), H->L+3 (11%)
5	3.71	0.045	H-2->L (66%), H-1->L (18%)
6	3.81	0.031	H-4->L (67%), H-3->L (22%)
7	3.89	0.026	H-L+3 (23%), H-1->L+1 (18%), H-4->L (17%), H-3->L (10%)
8	3.98	0.061	H-3->L (25%), H->L+2 (16%), H-5->L (14%)
9	4.02	0.053	H-5->L (49%)
10	4.07	0.095	H-5->L (23%), H->L+2 (15%), H->L+3 (15%), H-1->L+1 (14%)
11	4.08	0.007	H-2->L+1 (17%), H-4->L+1 (16%)
$^{3}T_{n}$	**E/eV**	**f_{osc}**	**MO contributions (> 10%)**
1	2.20	0.000	H->L (62%), H->L+1 (17%)
2	2.68	0.000	H-1->L (38%), H->L+1 (20%), H->L+2 (13%)
3	2.98	0.000	H->L (25%), H->L+1 (17%), H-1->L (11%)
4	3.16	0.000	H->L+1 (21%), H->L+3 (17%), H->L+2 (13%)
5	3.24	0.000	H->L+3 (26%), H-3->L (21%), H->L+2 (10%)
6	3.40	0.000	H-1->L+1 (23%), H-1->L (20%), H-3->L+2 (12%), H-1->L+3 (10%)
7	3.46	0.000	H-3->L (47%), H->L+2 (14%)
8	3.48	0.000	H-3->L+1 (18%), H-1->L+2 (15%), H-1->L+3 (14%), H-2->L (10%)
9	3.51	0.000	H-2->L (42%), H->L+2 (12%)
10	3.61	0.000	H-4->L+3 (37%), H-4->L+2 (16%), H-4->L+1 (13%)
11	3.70	0.000	H-4->L (26%), H-2->L (6%)
12	3.71	0.000	H-2->L+3 (13%), H-5->L+3 (12%)
13	3.81	0.000	H-4->L (50%)
14	3.86	0.000	H-5->L (51%)
15	3.99	0.000	H-1->L+1 (30%), H-1->L+3 (13%), H-7->L (11%)
16	4.10	0.000	H-2->L+1 (49%)

SOC	E/eV	f_{osc}	Singlet contributions (> 5%)	Triplet contributions (> 5%)
4	2.79	0.008	1 (11%)	2 (82%)
7	2.96	0.055	1 (64%)	2 (12%), 3 (11%)
9	2.99	0.007	1 (10%)	2 (5%), 3 (56%), 6 (9%)
14	3.27	0.005	2 (13%)	4 (19%), 5 (8%), 6 (16%), 8% (10%), 12 (8%)
16	3.33	0.006	2 (24%)	6 (7%), 8 (5%), 9(5%), 10(33), 12(9%)
19	3.40	0.006	6 (5%)	4 (10%), 5 (25%), 6 (18%), 8 (%), 10 (7%)
21	3.48	0.003	-	7 (30%), 11 (13%), 12 (5%), 13 (7%)
23	3.50	0.010	4 (9%)	7 (33%) ,13 (8%)
24	3.53	0.006	6 (6%)	9 (30%), 10 (14%),11 (9%)
27	3.57	0.013	4 (14%)	6 (26%), 8 (18%), 9 (8%)
28	3.60	0.005	12 (11%)	6 (3%), 10 (16%), 12 (25%)
31	3.63	0.004	-	6 (15%), 7 (32%), 8 (16%), 9 (17%)
32	3.68	0.051	2 (17%), 3 (31%), 4 (8%)	12 (8%)
33	3.72	0.095	3 (6%), 5 (34%)	7 (7%), 11 (8%), 13 (14%)

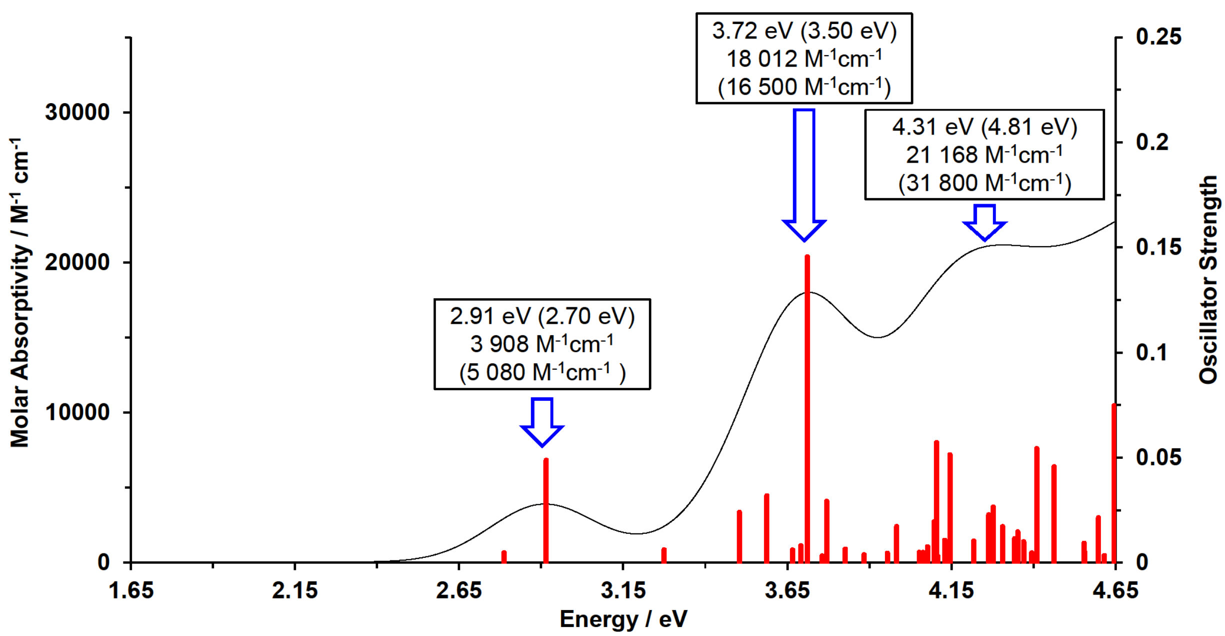

Figure S11. TDDFT simulated SOC-corrected spectrum (—), vertical excitations (—), and oscillator strengths of **3** in CH_2Cl_2. Calculated energies and molar absorptivities ($M^{-1}cm^{-1}$) at each peak maxima are shown with experimental (in parentheses).

Table S11. Spin-only and SOC-corrected TDDFT predicted singlet-singlet, singlet-triplet, and singlet-SOC vertical excitation energies (*f* > 0.003), MO contributions (>10%), singlet/triplet contributions (>5 %) for **3**. Entries in red reflect SOC calculated transitions which appear in valley regions of the absorption spectrum.

^1S_n	E/eV	f_{osc}	MO contributions (> 10%)	
1	2.82	0.065	H->L (97%)	
2	3.52	0.051	H->L+1 (75%), H-3->L (12%)	
3	3.71	0.080	H-1->L (44%), H-2->L (40%)	
4	3.73	0.024	H-4->L (44%), H-2->L (29%), H-1->L (11%)	
5	3.78	0.012	H-4->L (27%), H->L+2 (18%), H-3->L (15%), H-2->L (14%)	
6	3.86	0.177	H-2->L (23%), H-2->L (15%), H-1->L (14%), H-4->L (12%), H->L+2 (12%)	
7	3.87	0.003	H-5-> L (83%), H-4->L (14%)	
8	3.95	0.072	H-3->L (28%), H->L+4 (24%)	
9	4.04	0.125	H->L+2 (42%), H->L+4 (30%)	
^3T_n	**E/eV**	**f_{osc}**	**MO contributions (> 10%)**	
1	2.23	0.000	H->L (64%), H->L+1 (14%)	
2	2.68	0.000	H-1->L (61%)	
3	3.07	0.000	H->L+1 (45%), H->L (27%), H->L+2 (13%)	
4	3.23	0.000	H-3->L (33%), H->L+2 (20%)	
5	3.33	0.000	H->L+4 (44%), H-2->L+4 (14%), H-3->L (11%)	
6	3.43	0.000	H-3->L (22%), H-1->L (19%), H-3->L (18%), H->L+2 (15%)	
7	3.52	0.000	H-1->L+1 (21%), H-3->L (17%), H->L+2 (12%), H-3->L+2 (10%)	
8	3.57	0.000	H-2->L (67%)	
9	3.68	0.000	H-4->L (67%), H-5->L (11%)	
10	3.73	0.000	H-1->L+2 (25%), H-3->L+1 (18%), H->L+2 (11%)	
11	3.81	0.000	H-5->L (71%)	
12	3.89	0.000	H-4->L+4 (32%), H-1->L+4 (15%), H-4->L (11%)	
13	3.91	0.000	H-1->L+4 (24%), H-4->L+4 (16%), H-2->L+4 (15%)	
14	4.04	0.000	H-1->L+1 (30%), H-1->L+3 (12%), H-8->L (11%)	
15	4.06	0.000	H-5->L+4 (47%)	
SOC	**E/eV**	**f_{osc}**	**Singlet contributions (> 5%)**	**Triplet contributions (> 5%)**
4	2.79	0.005	1 (6%)	2 (90%)
7	2.92	0.049	1 (85%)	2 (6%), 9 (6%)
13	3.28	0.006	1 (85%)	3 (9%), 4 (29%), 5 (40%),
20	3.51	0.024	2 (19%), 3 (19%)	6 (7%), 9 (26%), 11 (8%)
24	3.59	0.032	2 (18%), 3 (19%), 5 (11%)	6 (6%), 9 (12%), 11 (6%)
27	3.67	0.006	-	7 (80%)
28	3.69	0.008	-	7 (74%), 10 (5%), 12 (6%), 13 (6%)
30	3.71	0.146	2 (12%), 4 (11%), 5 (8%), 6 (10%)	7 (12%), 9 (16%), 10 (5%), 11 (5%)

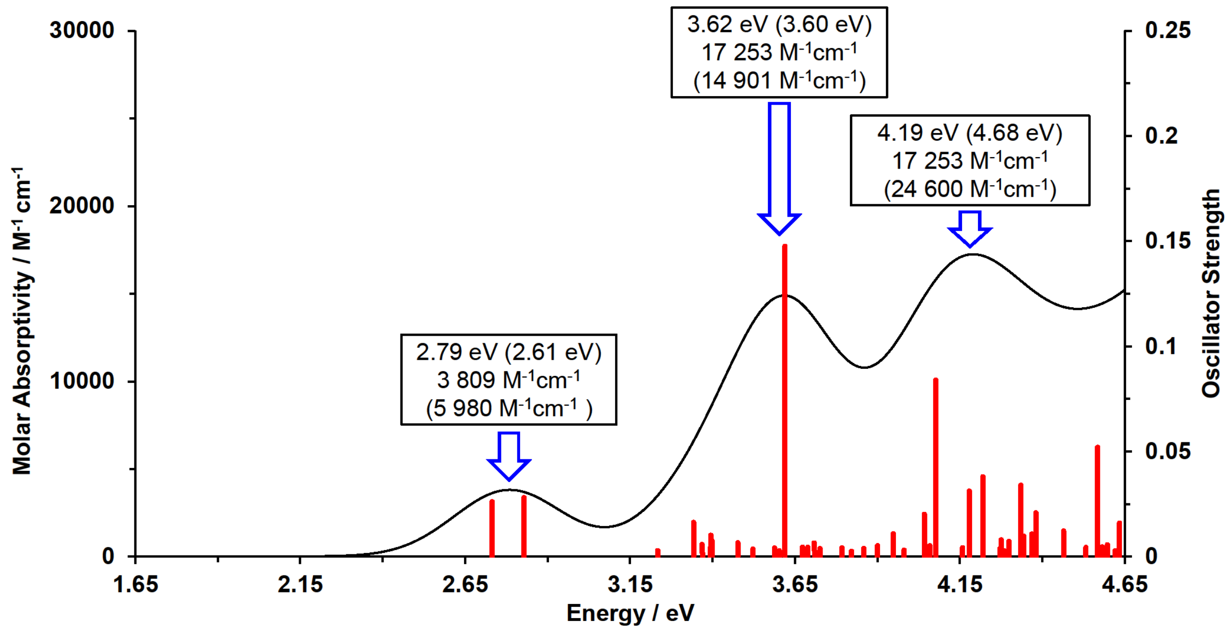

Figure S12. TDDFT simulated SOC-corrected spectrum (—), vertical excitations (—), and oscillator strengths of **4** in CH_2Cl_2. Calculated energies and molar absorptivities ($M^{-1}cm^{-1}$) at each peak maxima are shown with experimental (in parentheses).

Table S12. Spin-only and SOC-corrected TDDFT predicted singlet-singlet, singlet-triplet, and singlet-SOC vertical excitation energies (*f* > 0.003), MO contributions (>10%), singlet/triplet contributions (>5 %) for **4**. Entries in red reflect SOC calculated transitions which appear in valley regions of the absorption spectrum.

^1S_n	E/eV	f_{osc}	MO contributions (> 10%)
1	2.71	0.069	H->L (97%)
2	3.46	0.026	H->L+1 (67%), H-1->L (17%)
3	3.55	0.066	H-1->L (53%), H->L+1 (16%), H-2->L (16%), H-3->L (11%)
4	3.59	0.002	H-3->L (52%), H-2->L (45%)
5	3.67	0.080	H-4->L (30%), H-2->L (24%), H-3->L (18%), H-1->L (11%)
6	3.76	0.010	H->L+2 (46%), H-4->L (28%), H->L+4 (12%)
7	3.82	0.196	H-4->L (37%), H-3->L (13%), H-2->L (12%), H->L+2 (11%)
8	3.91	0.067	H-5->L (55%), H-1->L+1 (10%)
9	4.06	0.058	H->L+4 (55%), H->L+2 (24%)
^3T_n	**E/eV**	**f_{osc}**	**MO contributions (> 10%)**
1	2.17	0.000	H->L (69%)
2	2.68	0.000	H-1->L (55%)
3	2.99	0.000	H->L+1 (51%), H->L (22%)
4	3.2	0.000	H-5->L (32%), H->L+2 (23%)
5	3.32	0.000	H->L+4 (36%), H-5->L (26%)
6	3.4	0.000	H->L+2 (24%), H-5->L+1 (16%), H-2->L (14%), H-5->L (13%)
7	3.42	0.000	H-2->L (24%), H-1->L (18%)
8	3.52	0.000	H-3->L (49%)
9	3.59	0.000	H-3->L (34%), H-5->L (13%)
10	3.62	0.000	H-4->L (48%), H-2->L (24%)
11	3.71	0.000	H-1->L+2 (23%), H-4->L (17%), H-5->L+1 (17%)
12	3.86	0.000	H-1->L+4 (33%), H-3->L+4 (26%)
13	3.91	0.000	H-3->L+4 (35%), H-1->L+4 (20%)
14	3.99	0.000	H-1->L+1 (37%)
15	4.04	0.000	H-4->L+4 (34%), H-2->L+4 (22%)
16	4.09	0.000	H-2->L+1 (22%)

SOC	E/eV	f_{osc}	Singlet contributions (> 5%)	Triplet contributions (> 5%)
4	2.73	0.026	1 (41%)	2 (53%)
7	2.83	0.028	1 (49%)	2 (40%), 8 (6%)
13	3.24	0.003		4 (41%), 5 (30%)
14	3.34	0.016	2 (15%), 3 (21%)	6 (7%), 7 (15%), 8 (17%), 10 (5%)
16	3.37	0.006	2 (5%), 5 (5%)	7 (47%), 8 (14%), 9 (6%), 10 (5%)
18	3.40	0.004	-	4 (44%), 5 (37%), 7 (8%)
19	3.40	0.010	-	4 (28%), 5 (38%), 7 (13%)
20	3.40	0.008	-	4 (38%), 5 (35%)
23	3.48	0.007	-	6 (62%), 7 (9%), 8 (5%)
24	3.53	0.004	2 (22%), 3 (18%), 6 (8%)	6 (8%), 8 (13%), 10 (5%)
25	3.59	0.004	-	9 (8%), 11 (16%), 12 (25%), 13 (22%), 15 (9%)
26	3.60	0.003	2 (6%)	9 (9%), 11 (19%), 12 (22%) 13 (18%)
27	3.62	0.148	2 (18%), 4 (7%), 5 (11%), 7 (10%)	8 (10%), 9 (9%), 10 (6%)

Excited State Dynamics of 4

The excited state dynamics of **4** were explored using the ESD module implemented in Orca v. 4.2.1.[2,3] The average rates of ISC (5) and phosphorescence (6) were estimated using the following equations:

$$k^{ISC,aver.} = k^{ISC,-1} + k^{ISC,0} + k^{ISC,+1} \quad (5)$$

$$k^{Phos,aver.} = \frac{k_1 + k_2 e^{-\left(\frac{\Delta E_{1,2}}{k_B T}\right)} + k_3 e^{-\left(\frac{\Delta E_{1,3}}{k_B T}\right)}}{1 + e^{-\left(\frac{\Delta E_{1,2}}{k_B T}\right)} + e^{-\left(\frac{\Delta E_{1,3}}{k_B T}\right)}} \quad (6)$$

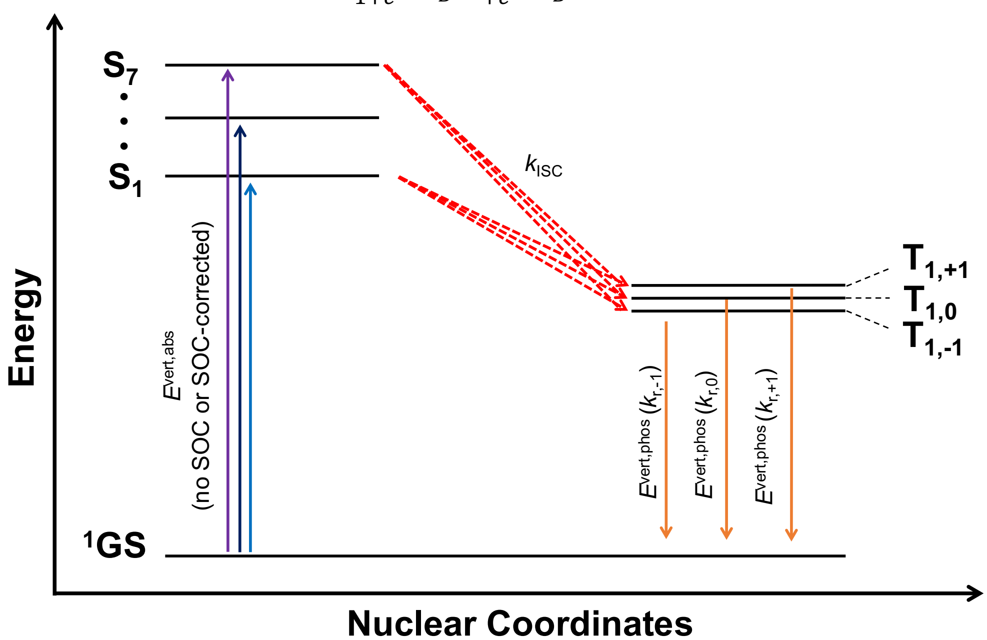

Figure S13. Schematic of photophysical processes and calculated parameters.

Table S13. Calculated rate of intersystem crossing from $^1S_1(^1GS_{eq})$ and $^1S_7(^1GS_{eq})$ to the three substates of $^3T_{1,eq}$ (M_S = -1, 0, +1) for **4** at 298 K and 77 K in CH_2Cl_2.

Temp / K	k_1 / s^{-1} M_S = -1	k_2 / s^{-1} M_S = 0	k_3 / s^{-1} M_S = +1	$k_{aver.}$ / s^{-1}
$S_1(^1GSeq) \rightarrow T_{1,M_S}(T_{1,eq})$	3.845×10^{12}	0	2.317×10^{13}	8.870×10^{12}
$S_7(^1GSeq) \rightarrow T_{1,M_S}(T_{1,eq})$	2.928×10^{13}	0	0	1.020×10^{13}

Table S14. Calculated phosphorescence parameters for **4** at 298 K and 77 K in CH_2Cl_2.

Temp / K	k_1 / s^{-1}	k_2 / s^{-1}	k_3 / s^{-1}	$k_{aver.}$ / s^{-1}
298	36 631	57 303	77 508	56 777
77	29 492	52 137	72 632	49 973

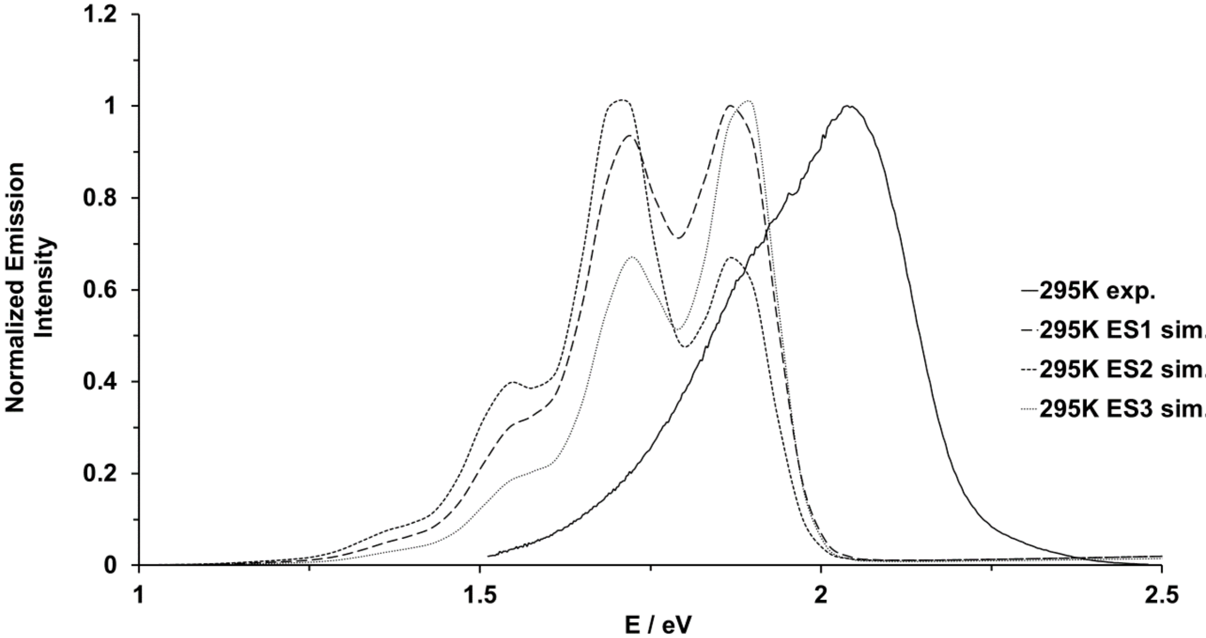

Figure S14. TDDFT simulated (FWHM = 3000 cm^{-1}, T = 298 K) and experimental (T = 295 K) phosphorescence spectra of **4** in CH_2Cl_2. The three substates (M_S = -1, 0, +1) of the lowest excited triplet state are considered.

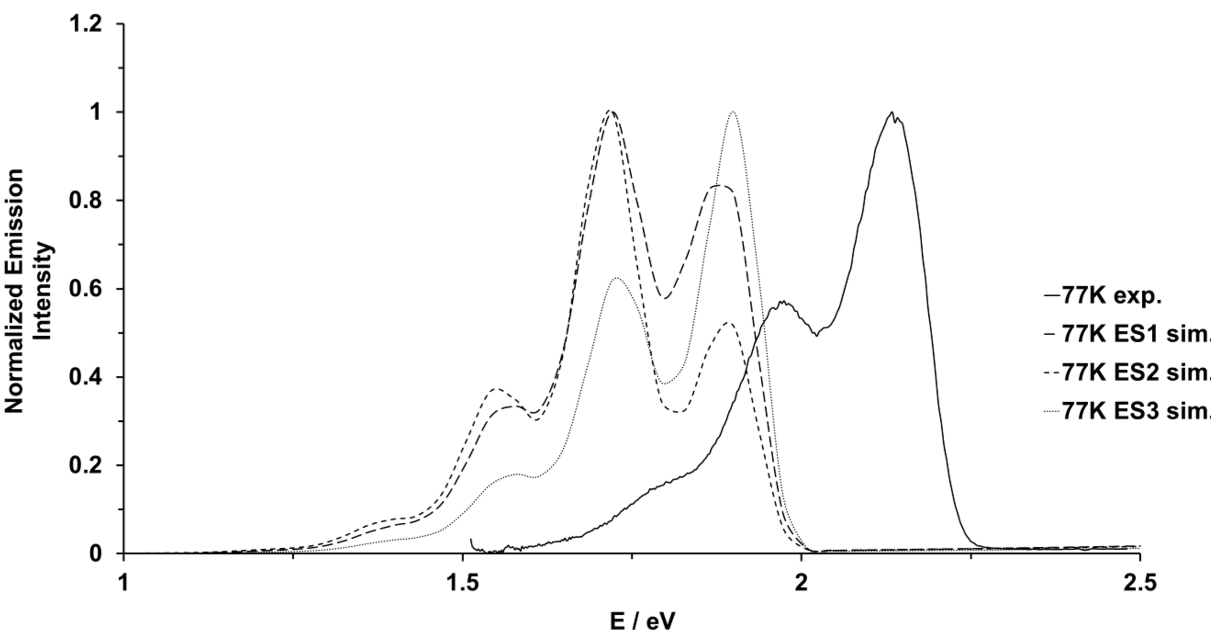

Figure S15. TDDFT simulated (FWHM = 3000 cm^{-1}, CH_2Cl_2) and experimental phosphorescence spectra of **4** at 77 K. The three substates (M_S = -1, 0, +1) of the lowest excited triplet state are considered.

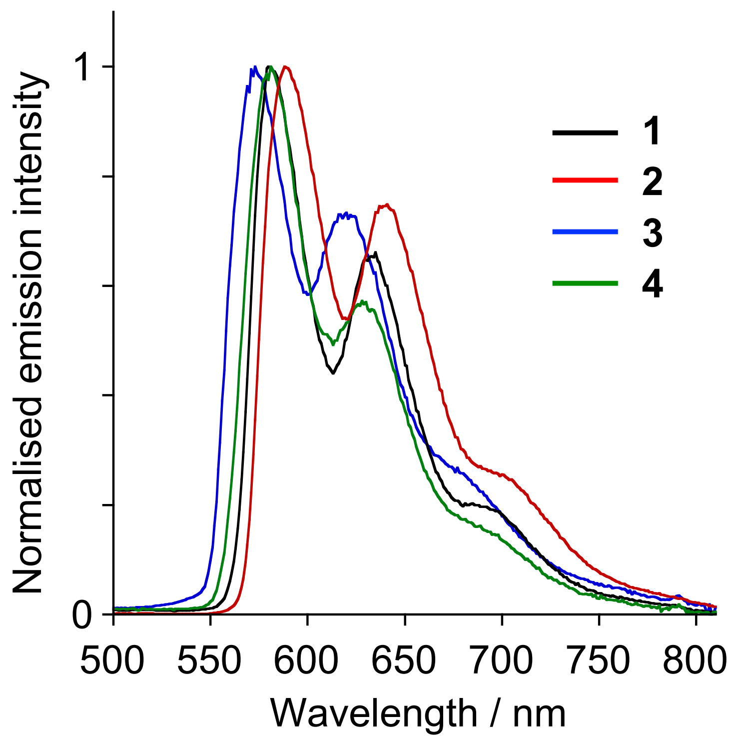

Figure S16. Stackplot of emission spectra of **1-4** in EPA (diethyl ether / isopentane /ethanol 2:2:1 v/v) at 77 K.

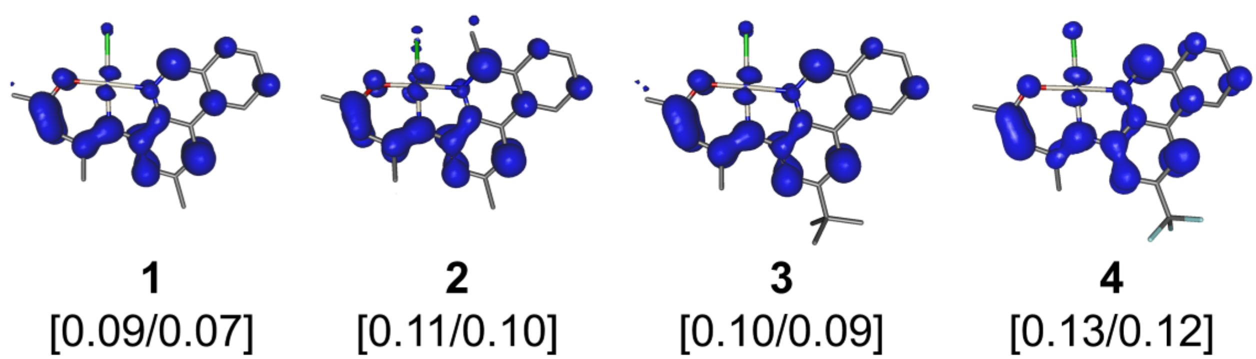

Figure S17. Spin density maps (isovalue = 0.004) of **1-4** at the equilibrium geometries of the lowest-lying excited triplet state. Shown in square brackets are the Löwdin/Mulliken spin densities on Pt.

NMR and HRMS Figures

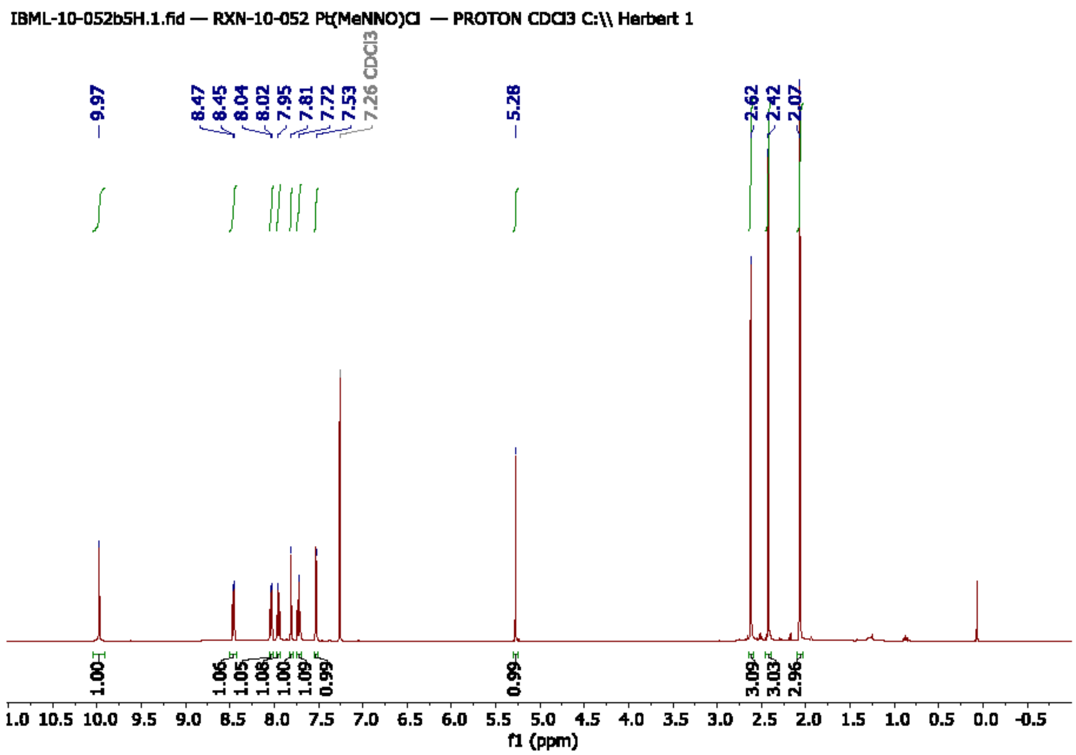

Figure S18. ^{1}H NMR (500 MHz, 25 °C) spectrum of **1** in $CDCl_3$.

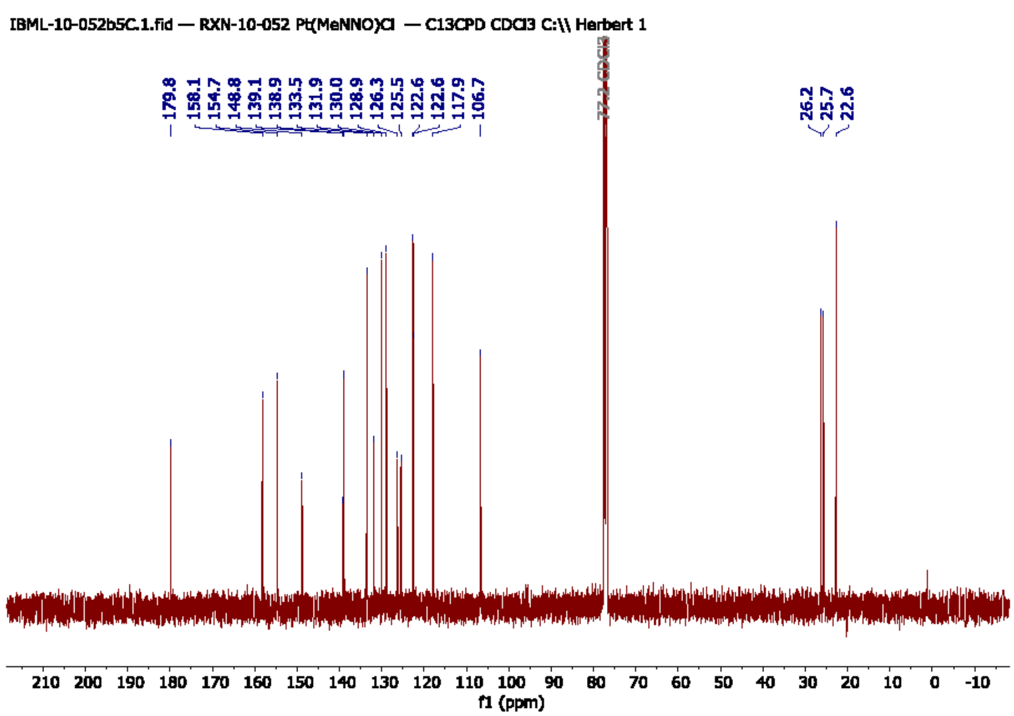

Figure S19. $^{13}C\{^{1}H\}$ NMR (125 MHz, 25 °C) spectrum of **1** in $CDCl_3$.

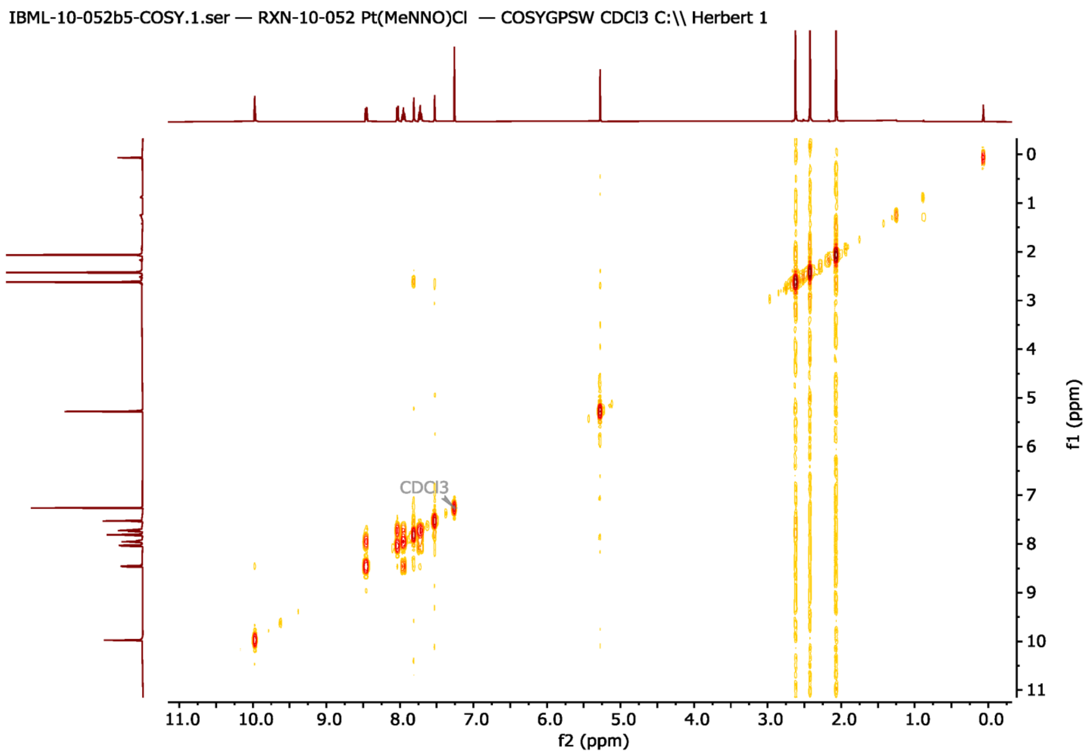

Figure S20. ^{1}H-^{1}H COSY spectrum of **1** in $CDCl_3$.

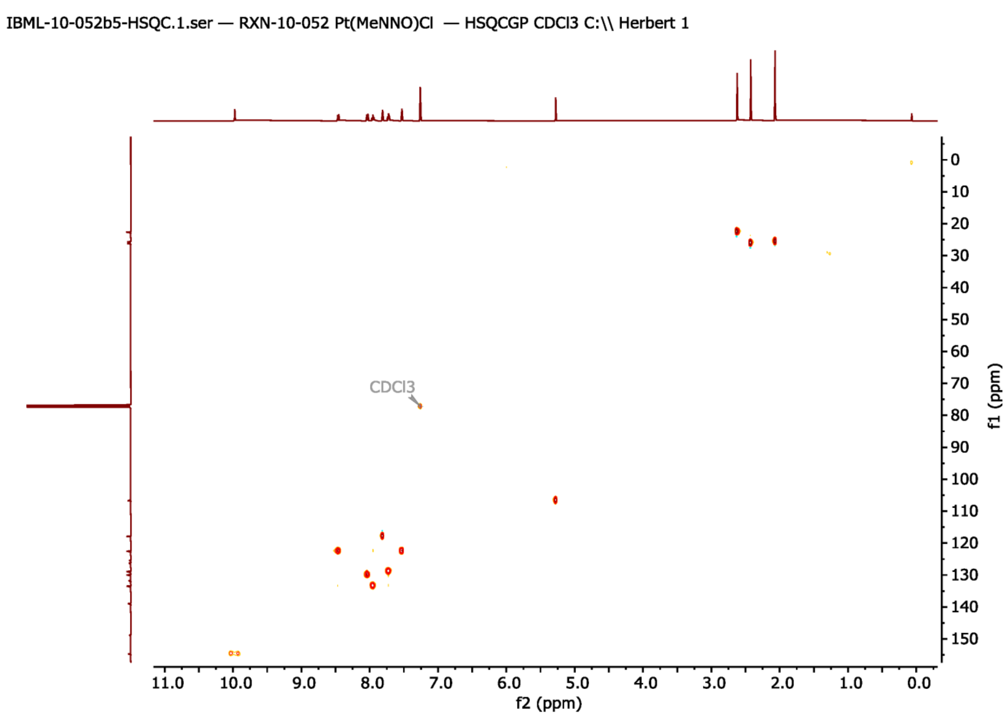

Figure S21. HSQC spectrum of **1** in $CDCl_3$.

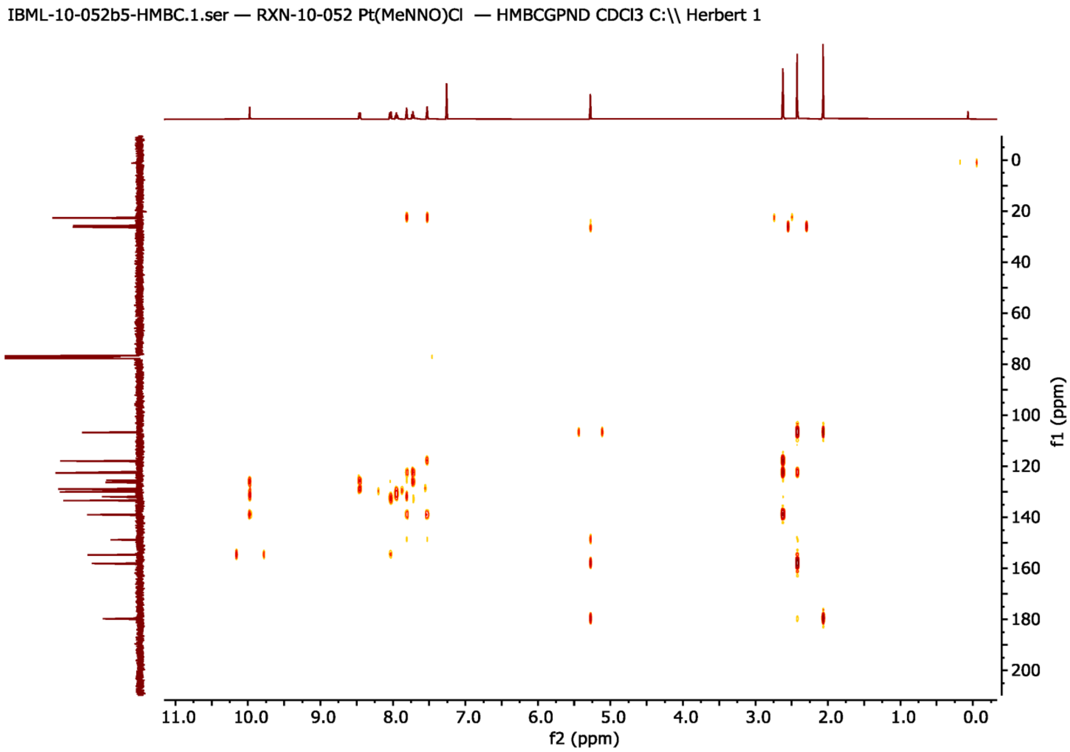

Figure S22. HMBC spectrum of **1** in $CDCl_3$.

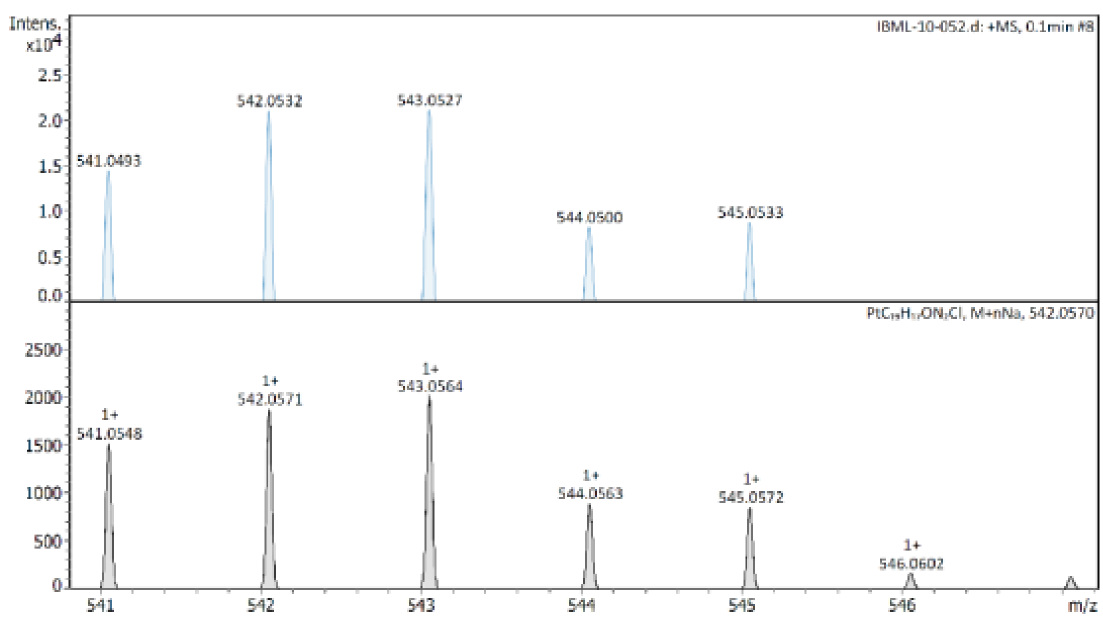

Figure S23. HRMS (ESI-TOF positive mode) of **1**.

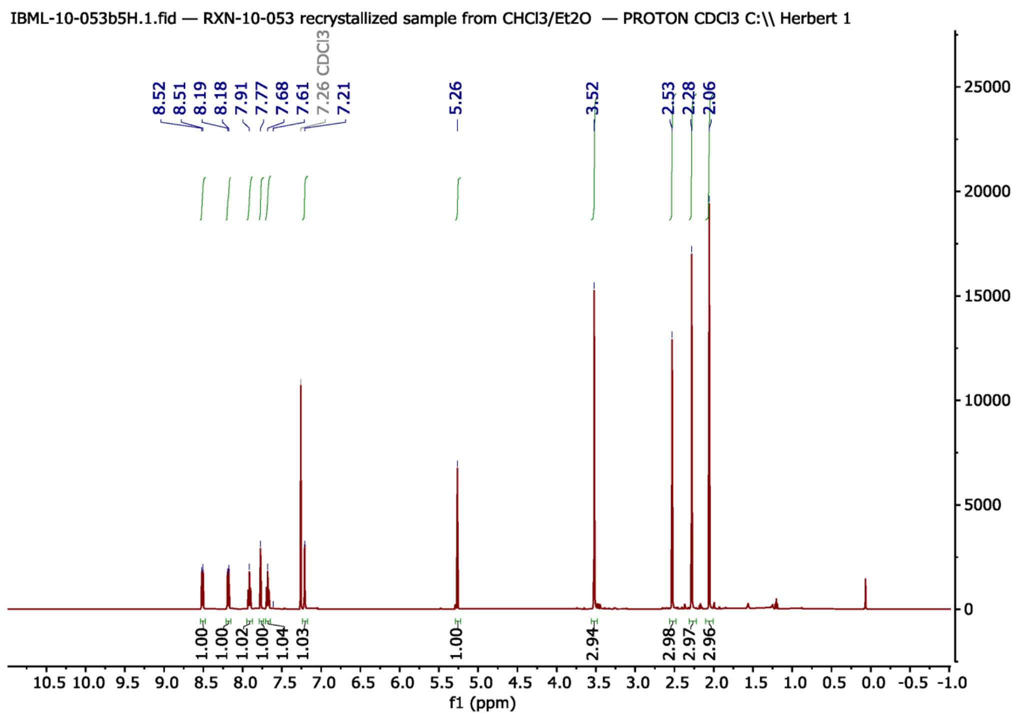

Figure S24. ^{1}H NMR (500 MHz, 25 °C) spectrum of **2** in $CDCl_3$.

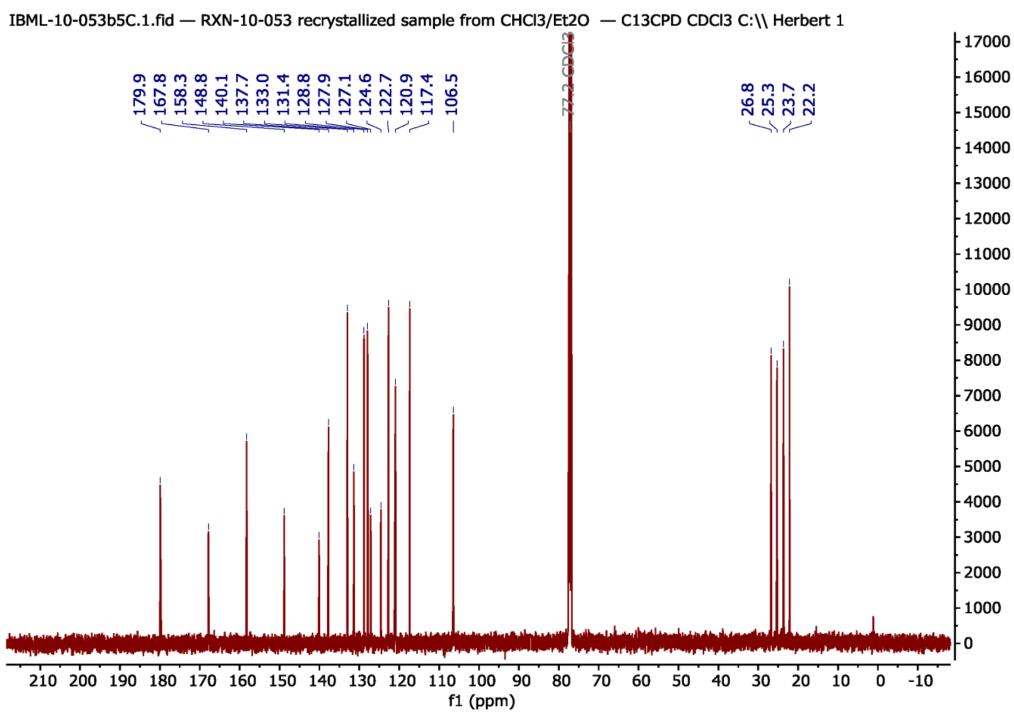

Figure S25. $^{13}C\{^{1}H\}$ NMR (125 MHz, 25 °C) spectrum of **2** in $CDCl_3$.

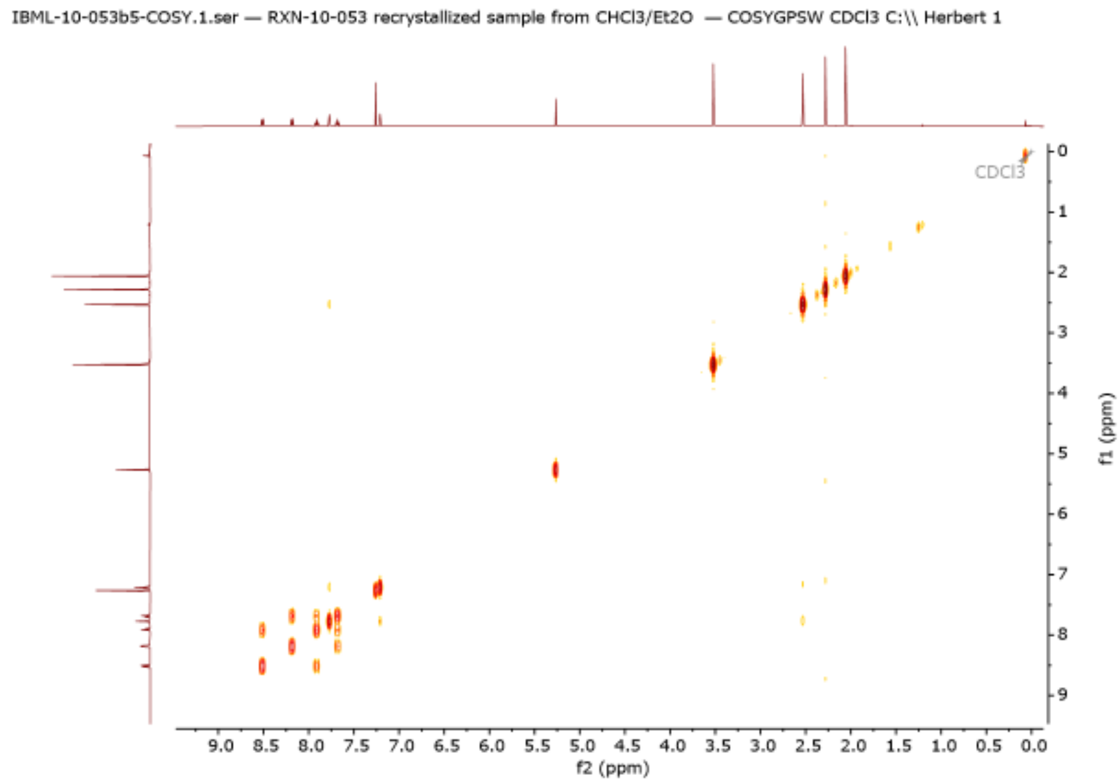

Figure S26. ^{1}H-^{1}H COSY spectrum of **2** in $CDCl_3$.

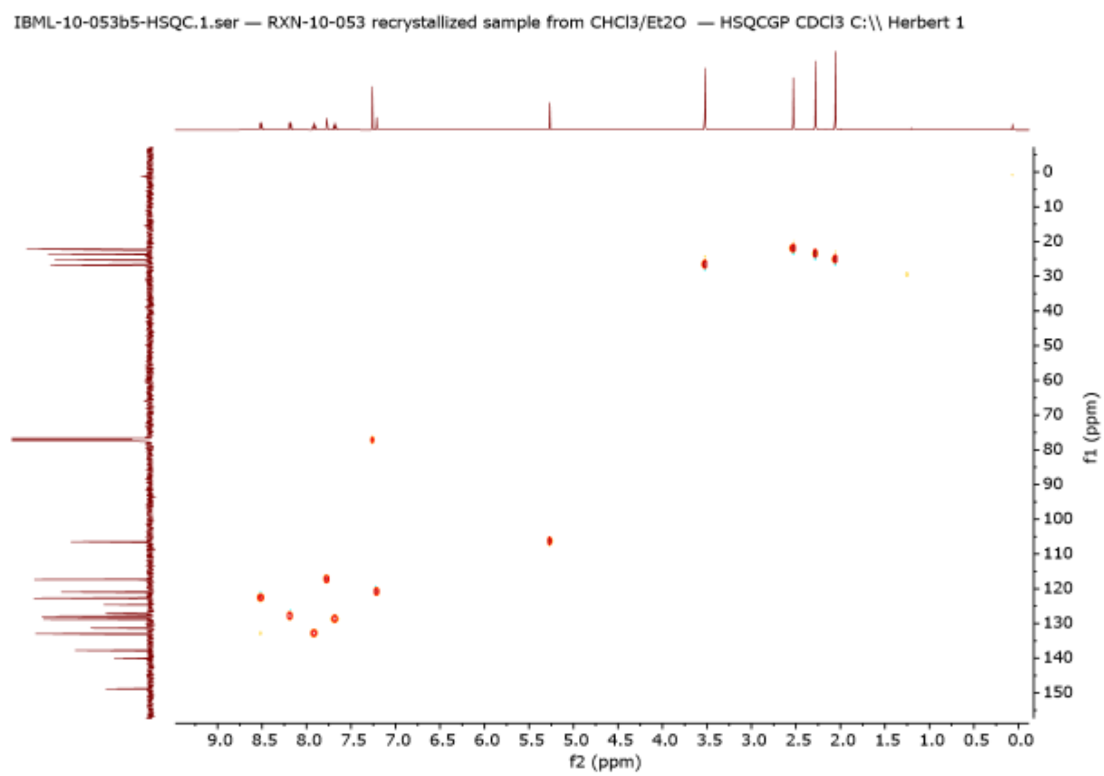

Figure S27. HSQC spectrum of **2** in $CDCl_3$.

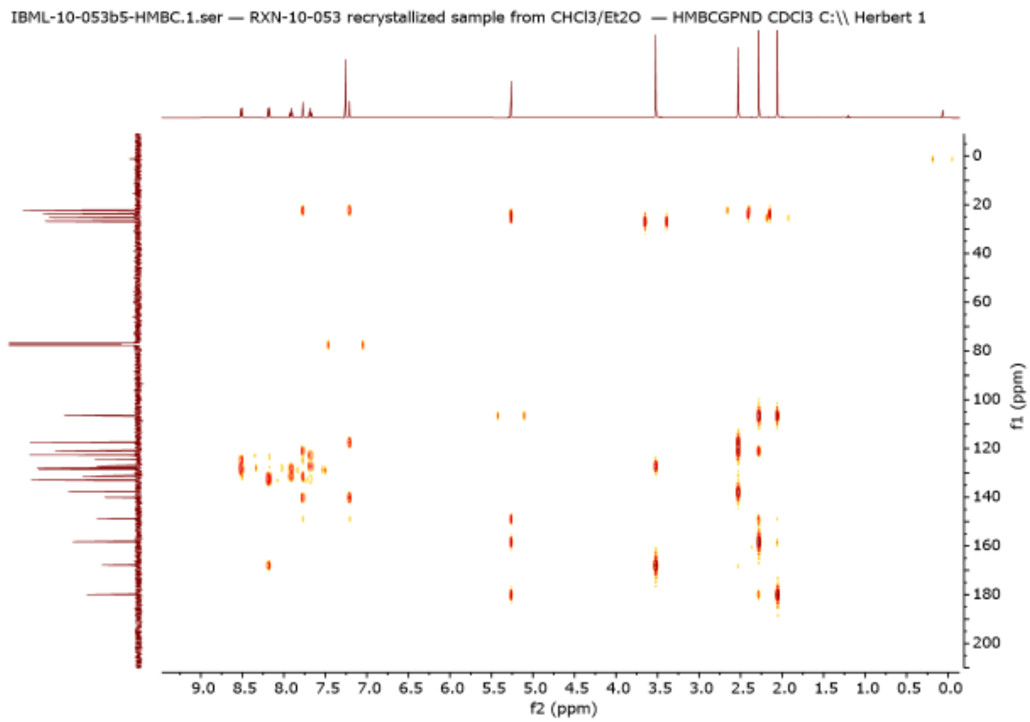

Figure S28. HMBC spectrum of **2** in $CDCl_3$.

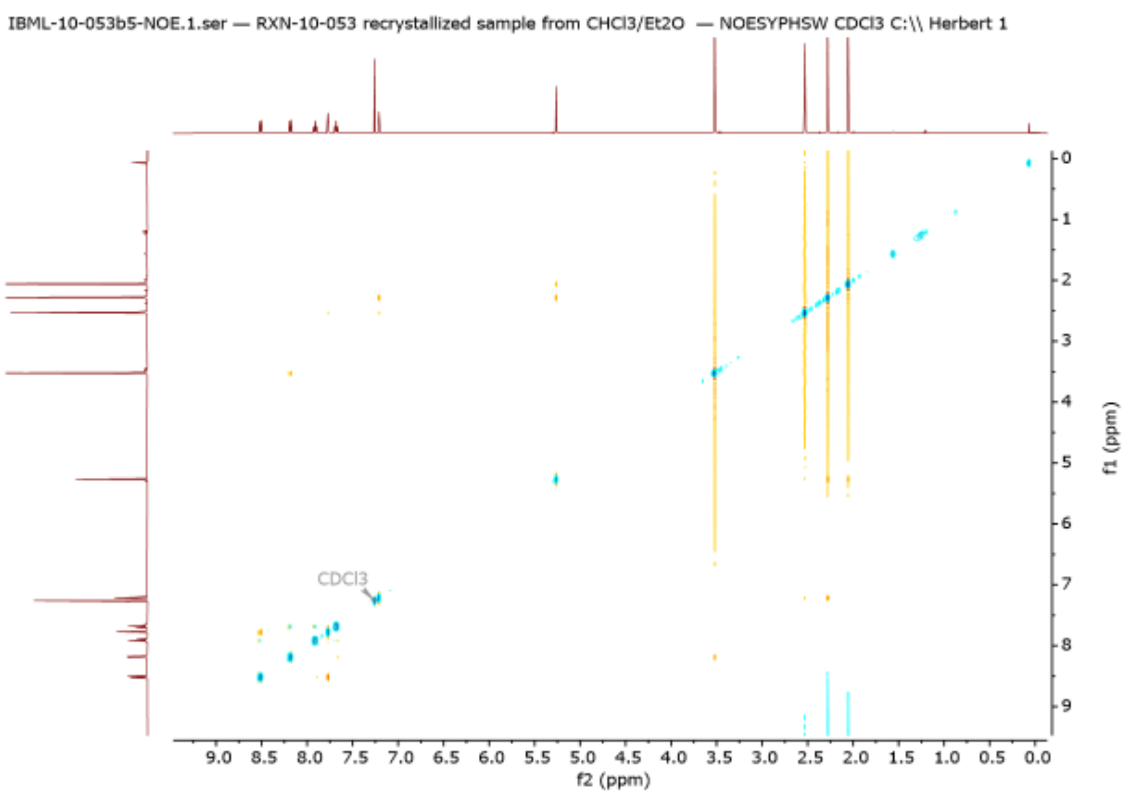

Figure S29. 2D-NOESY spectrum of **2** in $CDCl_3$.

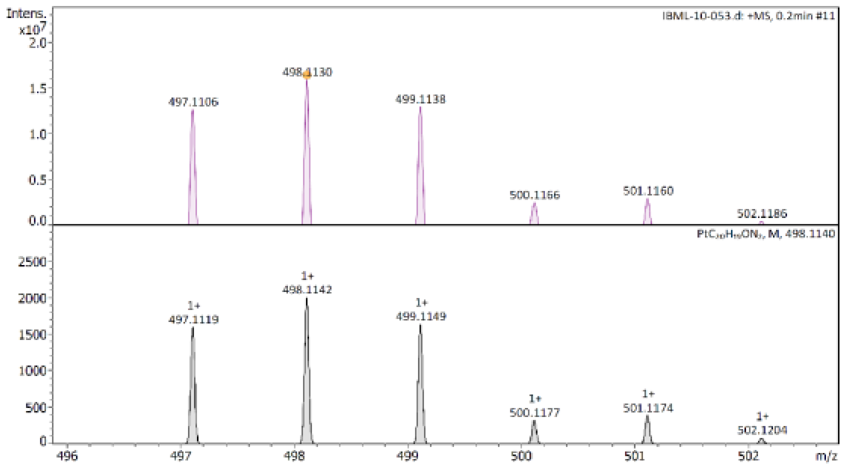

Figure S30. HRMS (ESI-TOF positive mode) of **2**.

Optimized Coordinates

1, $^{1}GS_{eq}$

C	3.64099155062907	7.71398624007048	8.54078991755222
H	3.66085520156593	6.81299740130944	7.93552098767605
C	3.52517291969900	7.66146048774590	9.95225738099578
C	3.43503552432320	6.42241075577230	10.60957427689913
H	3.44271994425982	5.51474619118351	10.01685875537876
C	3.34319906980158	6.37457065077047	11.97705022012024
H	3.27493556827839	5.42137386393497	12.48683935132515
C	3.33348658815265	7.56545129394147	12.71609904540491
H	3.26130327612409	7.52455183281692	13.79670107856893
C	3.40389136736768	8.78513741457966	12.08681772129385
H	3.38550071577152	9.68819589995348	12.68216890972175
C	3.49983071407732	8.86299067569080	10.68923190045281
C	3.55857459676318	10.10251134300020	9.95737804579744
C	3.69032703217882	10.04261646032461	8.56243557078316
C	3.75329981819312	11.21382043075438	7.76449160784690
C	3.55539101370367	12.42242930670397	8.41298816751185
H	3.46874806302513	13.34183896851751	7.86216555619912
C	3.43638630540878	12.50579150266752	9.80622237622328
C	3.46286123035922	11.36063223092182	10.56786094785203
H	3.36586633442455	11.43405259159642	11.64322933520231
C	3.25126010736515	13.85606750504569	10.42835149534051
C	4.60923032874852	13.33855705408571	5.85861518954927
H	3.70009421962398	13.93019740672750	5.99105319387207
H	5.17757065764593	13.79160267657216	5.04938171883164
H	5.19876753335655	13.40776840713657	6.77292929285516
C	4.29790072155575	11.91164360470463	5.49908871942725
C	4.43083327863673	11.62662967515458	4.13634243224913
H	4.68249001970100	12.47321115258357	3.51371275170261
C	4.31952216642510	10.41274009189892	3.45735999417389
C	4.50949788421026	10.39656866917849	1.97155975550439
H	5.30495285274161	9.69175178733749	1.72282263557927
H	4.75940864615190	11.38001244707317	1.57705169116120
H	3.59841339069812	10.03063174469488	1.49318216314858
Cl	3.87025691903977	6.75597072528886	5.49796090992141
N	3.73365252993340	8.83815181587929	7.88730425330608
N	3.96231517779865	10.99127398246282	6.40098676040653
O	4.09612422749563	9.27209685908492	3.96388088973166
Pt	3.90025698659982	9.03459450386048	5.92362364526763
H	3.86612193769574	14.60826903505056	9.93090616391603
H	3.51458840848721	13.84612984864107	11.48706009085698
H	2.21011517198218	14.18182546528196	10.34216510039252

1, $T_{1,eq}$

C	3.64091397656776	7.67001189027181	8.55988608524942
H	3.67259971019398	6.76913315725141	7.96229227634256
C	3.52698060249842	7.63566465472483	9.95320504067109
C	3.45098558970904	6.40525189060018	10.64699219755702
H	3.46942591175715	5.48456097789733	10.07505787503275
C	3.36112841243195	6.38268440740407	12.01091166586034
H	3.30473491039104	5.43646287921874	12.53577612566853
C	3.33681641967703	7.58631422691348	12.73950322591805

H	3.26603630097516	7.56102290982921	13.82030208480231
C	3.38980340491351	8.79244092154374	12.08542940258651
H	3.35897417851243	9.70599839449291	12.66523791593334
C	3.48119901873060	8.85140009204606	10.68638626377985
C	3.52170198345911	10.08298062387715	9.94460607816017
C	3.64801000023510	10.01005684820925	8.54399501474171
C	3.72994322909786	11.19492276365234	7.74356359634092
C	3.53679448009138	12.44573072621412	8.39787467289380
H	3.45498450609625	13.35548853498389	7.83043632318553
C	3.41362301636671	12.52301280771909	9.76230484926323
C	3.43644502068486	11.34846373189492	10.53254628321148
H	3.34580030421238	11.43236471007850	11.60799851042206
C	3.24977207104930	13.84648716011460	10.44416540247432
C	4.71248798231488	13.32746602095810	5.88571607430769
H	3.85276103045884	13.99044307655381	6.02050611583951
H	5.32017022805987	13.75194389044787	5.08804264516468
H	5.30444206270703	13.34936059377599	6.80085996655282
C	4.32012521355810	11.92932378252022	5.49908466509508
C	4.40845733396529	11.64420591691558	4.14199380531090
H	4.66424461504942	12.49381335054412	3.52196038722582
C	4.28796392252438	10.43542937545639	3.43648319037850
C	4.48554655608789	10.41486925019137	1.95524856368972
H	5.29576007553664	9.72393803291537	1.70977224836937
H	4.72475877715622	11.40081830464453	1.55935095248660
H	3.58659087514616	10.03488857695199	1.46335352344259
Cl	3.87594012279591	6.80627155449541	5.44052218038795
N	3.71111567523292	8.82364282784933	7.88606813278310
N	3.96769767229409	10.97214904435962	6.42221238206013
O	4.05955709408080	9.30027668957170	3.96247978209230
Pt	3.90539129732753	9.04180346274666	5.92487728347829
H	3.41871428518887	14.67182126192055	9.75142845816511
H	3.95966480705470	13.94782968434437	11.26861821672864
H	2.24794732580931	13.95610099389907	10.87014053634599

2, $^{1}GS_{eq}$

C	3.64851325668671	7.71266951215108	8.52508055200103
C	3.88807931521629	6.42881648625052	7.81335003273100
C	3.58800052669988	7.70551837388345	9.96579594360683
C	3.62930572037754	6.49268023451959	10.67824028209702
H	3.70574685552652	5.55937394513205	10.13888597183793
C	3.56276219566733	6.47623212244049	12.04887927833768
H	3.59062046268635	5.53285641063186	12.58057702062919
C	3.46344511453666	7.67777964806296	12.75685835905642
H	3.42620154437715	7.66609342103393	13.83990347583838
C	3.40783653610696	8.87272161129748	12.08213032821888
H	3.33179615479889	9.79295120440001	12.64519561282152
C	3.45916139597048	8.91280175668424	10.67985708634212
C	3.42380817677616	10.13983962617125	9.92927656787276
C	3.52484867060562	10.05083118739565	8.53789307884323
C	3.64834072973710	11.22266472886755	7.74996879408454
C	3.42396537164237	12.44180010048457	8.36250347612368
H	3.36505708727287	13.34467763084438	7.77636691152589
C	3.24776712385370	12.54363557116875	9.74709257725506
C	3.29352771750121	11.40627338734430	10.52013135223583
H	3.18647950189488	11.49070336802249	11.59352949482810
C	3.00497202648131	13.89447112123509	10.34587738919222

C	5.00096743785895	13.22298730996484	6.01902358459534
H	4.21058383359562	13.97655351313282	5.96912812918092
H	5.79074602092890	13.54172972996127	5.34070953926442
H	5.39357215685861	13.20506374058769	7.03496380356333
C	4.49328596469991	11.88139948222258	5.57289325460537
C	4.66216322474139	11.61116793034933	4.21052213651168
H	5.19613300815954	12.36114714049608	3.64438074081685
C	4.18880973290372	10.52413005440378	3.47687410710691
C	4.49491655382923	10.44783360911215	2.01211630392820
H	5.24843407286972	9.67063435145449	1.85796997103555
H	4.87838053205498	11.38823933583425	1.61922254891509
H	3.60412503761921	10.14087493046798	1.46308867284378
Cl	2.39976893307205	7.18912738525230	5.18085656599433
N	3.54380373647073	8.84003259803988	7.85719930893272
N	3.96147288563814	11.00077554616816	6.41088965309364
O	3.52096860673387	9.53706706651875	3.91465199748606
Pt	3.41606325638520	9.15904038301863	5.86156295973470
H	3.60606317247858	14.65996885003727	9.85202414604536
H	3.24193661475896	13.90647252761642	11.41075472606308
H	1.95563823463443	14.18275023932033	10.22894136278222
H	4.17455677406195	6.60029666945569	6.78193948642442
H	2.98925736518879	5.80966382795414	7.79601214914481
H	4.67665736004126	5.87963233060868	8.33133126645131

2, $T_{1,eq}$

C	3.65966039438627	7.67608662919302	8.55717800342449
C	3.93963671416907	6.40947617526546	7.83067068306883
C	3.58102687432862	7.68398935044045	9.97135946523786
C	3.63272238763062	6.47810528557361	10.71200851341812
H	3.71765080409112	5.53703885939974	10.18719150451955
C	3.55945733109970	6.48180649586038	12.07821098359866
H	3.59284003035960	5.54495049312550	12.62167151039238
C	3.44318050605203	7.69266776032831	12.77755261201097
H	3.39815762561277	7.69251326297658	13.85994818305805
C	3.37890246403673	8.87655518543012	12.08464585635125
H	3.28830309082016	9.80300339914190	12.63653016823383
C	3.43337528829812	8.90390969089044	10.68287557717897
C	3.39724987628178	10.12444224783756	9.92454346017067
C	3.49384140587372	10.02183118525035	8.52636452464228
C	3.63894742172280	11.20389382706056	7.72926088692401
C	3.42550396590873	12.46680914241154	8.34529255412375
H	3.36233100241047	13.35782444576837	7.74103662754079
C	3.24612785135266	12.56405631492564	9.70050017293039
C	3.28525828908591	11.39861444428228	10.48850575797130
H	3.19031286834937	11.49911618368005	11.56203280754374
C	3.01304290599774	13.89064087971501	10.35348852142189
C	5.11279888016230	13.17108887770981	6.05612624845374
H	4.40001496811664	14.00160895393731	6.05976520417256
H	5.92423159192091	13.45068925200262	5.38425739983672
H	5.51992499339655	13.07087736236970	7.06183005345134
C	4.50039757672888	11.89305149315028	5.56671379774208
C	4.58645442321163	11.64859547395230	4.20355109137882
H	5.08092077637655	12.42196644767984	3.62939114358549
C	4.14694799917579	10.54649325431911	3.45637237870100
C	4.43735878272939	10.47621588641250	1.99150670041186
H	5.20357004239526	9.71495955377657	1.81529209922704

H	4.79703227463906	11.42629107139667	1.59813174041529
H	3.54669334721737	10.15936529817604	1.44596532204161
Cl	2.43226902272523	7.21455910763568	5.19471327570492
N	3.52785204841502	8.83061546258896	7.86893675042720
N	3.96853872272170	10.97185369424605	6.43329438471002
O	3.53736124684609	9.53120014622489	3.92931876835160
Pt	3.46090299267843	9.14491426895737	5.87670544938700
H	3.21424993681458	14.71090777209485	9.66356480336011
H	3.65933237168864	14.01396396667442	11.22560504033462
H	1.98060359417832	13.98471755811208	10.70417316517385
H	4.32933858940102	6.60835727267220	6.83741500137132
H	3.04012408321658	5.80259695996806	7.70209201262192
H	4.67450263737563	5.82436960738467	8.38552979537713

3, $^{1}GS_{eq}$

C	3.63309876697858	7.71467978194245	8.53566820195441
H	3.65254189990948	6.81412800452090	7.92985853747364
C	3.51069284194698	7.66174958261916	9.94663115470897
C	3.41524283204441	6.42458229463876	10.60707885599846
H	3.42149778987652	5.51520444778925	10.01718223520350
C	3.32037684833601	6.38089353238027	11.97453355540540
H	3.24796130162703	5.42948571381678	12.48683517795394
C	3.31342549877018	7.57333384120965	12.71157274751476
H	3.24079405216783	7.53562201856458	13.79224043399303
C	3.38730665082665	8.79086034715328	12.07966756344297
H	3.37160819464174	9.69559008745233	12.67259869629269
C	3.48471042895525	8.86382581162792	10.68180644616068
C	3.54608595348536	10.10015277983287	9.94814035739757
C	3.69002610948177	10.04276198191533	8.55734073155037
C	3.75842990205322	11.21880664943414	7.76680230923542
C	3.55396468802609	12.42392719669768	8.42032222915993
H	3.47284960548119	13.33745124031774	7.86059896963927
C	3.41542174763666	12.50746562351333	9.81615886876051
C	3.43531389879306	11.35398209618585	10.56320601373179
H	3.32409616214977	11.40374725245217	11.63486761987389
C	3.25511744993096	13.87995072649693	10.45789656857912
C	3.07604235598067	13.78246401403308	11.96885348526422
H	2.19842292311133	13.18798061694272	12.23383106239741
H	2.93317763247388	14.78223659297844	12.38455581720917
H	3.95050685950790	13.34207000277388	12.45396021925814
C	4.50586786801505	14.71543580162782	10.16979631930683
H	4.41495901129889	15.70342959856343	10.62872597241744
H	4.66104223843714	14.85562960397755	9.09784524829380
H	5.39632789869339	14.23170868650318	10.57831476351681
C	2.02063136022939	14.58091576702368	9.88530485841631
H	1.11919893242125	13.99800907792804	10.08572082842508
H	2.09356996498515	14.73352977453187	8.80669980081277
H	1.90477457140694	15.56287447891175	10.35196792859567
C	4.61167022730586	13.34243858211688	5.85619626710680
H	3.69822421045143	13.92814784997776	5.98710083310270
H	5.17794881208367	13.79891171584505	5.04727276343781
H	5.20094961154978	13.41517385484596	6.77080426319732
C	4.30955135094586	11.91346266609191	5.49764046706451
C	4.45070877199868	11.62588568605235	4.13501723282068
H	4.70468166582903	12.47161447206729	3.51201629834771
C	4.34245178685258	10.41158211068011	3.45643242348351

C	4.53715254301178	10.38949829308176	1.97103532731668
H	5.32608669837600	9.67577760706419	1.72683962131623
H	4.79711832887111	11.36877143945495	1.57276164524153
H	3.62404028501575	10.02975214113190	1.49148439740682
Cl	3.87661757612168	6.75958989446126	5.49338406787937
N	3.73367539579605	8.83897401282464	7.88235093524387
N	3.97207334567689	10.99611643105852	6.40102580302892
O	4.11548822204841	9.27184989352942	3.96364712175399
Pt	3.90997692838556	9.03776832335864	5.92160695430702

3, $T_{1.eq}$

C	3.64633453490927	7.66357541993194	8.55962202379141
H	3.67489768436670	6.76088303214151	7.96427434196548
C	3.52977587585130	7.63117659053399	9.95498500174650
C	3.44812832185045	6.40325053407809	10.65118777913607
H	3.46189582154668	5.48087703163178	10.08195139395335
C	3.35809246841266	6.38444666082757	12.01564716926493
H	3.29688969299489	5.43995076471670	12.54292235125921
C	3.34065767212684	7.58941066036731	12.74146247813111
H	3.27301982579173	7.56702545045628	13.82257534110169
C	3.39688169780955	8.79377897500719	12.08477808591018
H	3.37227792018761	9.70891189949718	12.66241963631475
C	3.48579787352293	8.84795707840403	10.68507092389722
C	3.52373179595987	10.07602619588273	9.93973447457845
C	3.65714894093608	10.00118212147220	8.54508282810719
C	3.73472246122678	11.18666707521935	7.74884483301695
C	3.52575163689432	12.42981267890656	8.40128366793852
H	3.44297412171394	13.33091116765666	7.82115209810277
C	3.38986897694086	12.51442734043064	9.77268259333766
C	3.41736561577478	11.34190083227394	10.53121516222659
H	3.31352778149815	11.40254234722336	11.60308770914225
C	3.22883133939180	13.88231530883054	10.42991130734524
C	3.02649306667281	13.77126169263354	11.93770760203207
H	2.14300738726367	13.17798064101761	12.18545442288256
H	2.88167991845698	14.76839893126174	12.35930260322553
H	3.89181647497756	13.32434505196743	12.43310325406126
C	4.49136491938770	14.70963744485384	10.17068493262820
H	4.40537170160893	15.69325882679111	10.64045670208501
H	4.66104512844386	14.85895471316782	9.10206412322530
H	5.37154908748880	14.21157361171552	10.58443857482558
C	2.01029932327576	14.60217025859250	9.84835254638020
H	1.10039442838800	14.02628195939966	10.02983873534081
H	2.10095541656792	14.76415598152350	8.77233588630294
H	1.89713421643395	15.58092710858389	10.32280663895843
C	4.74825147921624	13.32077129270150	5.90889048901052
H	3.89995255274554	14.00061817035610	6.03748165536557
H	5.37364333588490	13.73919690471227	5.12131907071066
H	5.33084644316344	13.32715213102885	6.83091299723726
C	4.33639275820717	11.93240018627725	5.50821296391323
C	4.41847006468914	11.65329170473040	4.14899266665243
H	4.68147413702893	12.50342248709294	3.53213577667494
C	4.28284161612422	10.44951255463911	3.43891972767481
C	4.46889859080442	10.42737294755976	1.95645094748444
H	5.26160545856527	9.71935752919257	1.70260830397417
H	4.72636722196988	11.40875077043276	1.56030476989092
H	3.55808553396185	10.06829362819237	1.46996848111966

Cl	3.87638190137096	6.80846442789334	5.43121005248573
N	3.72163516593372	8.81278069081622	7.88578560345559
N	3.97494632353702	10.96810496841360	6.42548277618416
O	4.04461756741880	9.31277112062773	3.96396584209278
Pt	3.90940672070506	9.04156309833444	5.92412065385682

4, $^{1}GS_{eq}$

Pt	-0.96226595637032	7.13778197321001	6.38922367143552
Cl	-1.17296189762445	6.40908104337367	4.20586357465322
O	-2.30155231566984	8.52382717404969	5.92982684545189
F	2.80004853061459	8.21856758689376	12.05249516587666
N	0.28490977427578	5.70405891159499	6.93713385767357
F	2.22636226417775	6.30722830730120	12.86241132300655
F	4.08972568372262	6.49893005873586	11.79213385567979
N	-0.64114962422141	7.75067467172971	8.27835470453079
C	0.84980052383339	5.90892090667714	8.18059564545259
C	0.41288045728918	7.06373970877996	8.88101271873311
C	-1.43392681207611	8.64927497483204	8.86097026579113
C	0.55060675975264	4.62112489038430	6.26369495909006
H	0.06825991060969	4.53694010204444	5.29504818157652
C	1.10744276998996	7.39134843407339	10.03798531385136
H	0.91868822926584	8.30858370608997	10.56596776334474
C	1.80727542670003	5.02731761027272	8.70115009482210
C	2.11215230626341	6.55195376823616	10.52136809014519
C	2.07184220745335	3.80402406995750	7.98533877206403
C	2.44674938923153	5.37545805573353	9.89652587260592
H	3.22147858644831	4.74806904344612	10.31305685413813
C	1.35146250673182	8.96260445500081	10.32729060727195
H	1.18904896893136	8.06528988612976	10.92471182410054
H	2.28061396540341	9.42992817785873	10.64615909863772
H	0.54573699184533	9.66890739776317	10.54352084360114
C	1.41041381213051	3.60815013643400	6.75593537486052
C	2.81042924578362	6.90130606447141	11.80587258600689
C	-2.79187774232458	9.28191675380265	6.81829672533018
C	1.59157544122375	2.41880083983065	6.03158180468520
H	1.06382992519285	2.28920543884662	5.09353323920213
C	-2.43112251098611	9.34102057649488	8.16826403015225
H	-3.01090166281420	10.03193007896508	8.76402439922227
C	-3.87889525894099	10.17852519978855	6.31219287984419
H	-3.45253312362735	10.87075604417254	5.58214150397200
H	-4.35832818050329	10.74484690999119	7.10933831708839
H	-4.62158910692564	9.57182592357661	5.78991263158977
C	2.91304292719491	2.78751207904972	8.45689347140472
H	3.42917050530854	2.89944339918419	9.40128695809309
C	2.41043974793522	1.43417609556905	6.52082350401325
H	2.54558631723850	0.51164061308731	5.96988922062843
C	3.07283633343396	1.62525314818646	7.74065728660266
H	3.71571954992625	0.84515578438016	8.13111616376953

4, $T_{1,eq}$

Pt	-1.02873065408422	7.07947864640683	6.42895437666489
Cl	-1.29210639561141	6.38247141831623	4.27807792329788
O	-2.34937864969681	8.49024219177852	5.97147073826593
F	2.77060402443182	8.26769947519690	12.03612854116537
N	0.25924265397903	5.66466508559823	6.94071559388038

F	2.23998838759950	6.34239673569277	12.84193291429871
F	4.08639966433209	6.56949500869028	11.75033646384569
N	-0.66597372817022	7.70066907218112	8.27542609133256
C	0.83034714470056	5.88540981993157	8.14690824811893
C	0.38943345520273	7.04864517355423	8.85681218838578
C	-1.44968811804705	8.64533150271019	8.87988583985351
C	0.52050838251212	4.54310450625611	6.25417559473256
H	0.02219620921236	4.44017860971697	5.30091023007089
C	1.10035538441512	7.41349585780629	10.02551874717832
H	0.90785194835214	8.34418522071257	10.52844578358764
C	1.79670084515581	5.01225490863512	8.68668156805863
C	2.09264495669769	6.59855286104675	10.50467622558524
C	2.06880383013080	3.78618279508212	7.97813402408787
C	2.42276885637776	5.38824868592598	9.87575325224026
H	3.19588716308002	4.76778703764172	10.30592318695975
C	-1.40161703033403	8.88574312087699	10.35956840604453
H	-1.25639173351523	7.95724168053235	10.91256913123283
H	-2.34443866377429	9.32834001886106	10.67702928345111
H	-0.61046272986985	9.58168296679023	10.65297932034614
C	1.39433684853244	3.57108628832989	6.74550583607305
C	2.79921704952203	6.95185067219460	11.77753142372482
C	-2.78208199695624	9.32593998788848	6.82276948699627
C	1.61518093045120	2.37053760262673	6.03264130555417
H	1.08779074409255	2.21535887662342	5.09809958719719
C	-2.38147426364449	9.39286869688300	8.17027070961523
H	-2.91608394029877	10.12669236761917	8.76000363781316
C	-3.81648156769844	10.27096847717369	6.30442190774370
H	-3.35261459674420	10.95284460566830	5.58560299476068
H	-4.27799942144244	10.85591284041680	7.09931158541122
H	-4.58332832042963	9.70648974537762	5.76956791643698
C	2.93522220687856	2.79164970421365	8.45052360238460
H	3.45168525859814	2.92465904427728	9.39268154069829
C	2.46746939903039	1.42074856731160	6.52088696359868
H	2.63052406434206	0.50236470658321	5.96957261656162
C	3.13197940149072	1.63040663546990	7.74278335425634
H	3.79901300119964	0.87121878140100	8.13241185848802

REFERENCES

(1) Pan, L.; Hu, B.; Zhu, X.; Chen, X.; Shang, J.; Tan, H.; Xue, W.; Zhu, Y.; Liu, G.; Li, R.-W. Role of Oxadiazole Moiety in Different D–A Polyazothines and Related Resistive Switching Properties. *J. Mater. Chem. C* **2013**, *1*, 4556.

(2) Neese, F. The ORCA Program System. *WIREs Comput. Mol. Sci.* **2012**, *2*, 73–78.

(3) Neese, F. Software Update: The ORCA Program System, Version 4.0. *WIREs Comput. Mol. Sci.* **2018**, *8*, e1327.